

**A THEOREYICAL AND EXPERIMENTAL ANALYSIS
OF TRANSIANT OPERATION OF A SMALL SCALE
REFRIGERTION SYSTEM**

ATHESIS

SUBMITTED TO THE COLLEGE OF ENGINEERING

UNIVERSITY OF BABYLON IN PARTIAL

FULFILMENT OF THE REQUIREMENTS FOR THE MASTER OF SCIENCE DEGREE

IN MECHANICAL ENGINEERING (POWER)

BY

ZEHRA HAMOD GELHAM

B.Sc.(Mech. Eng.) 1997

JANUARY 2006

بِسْمِ اللَّهِ الرَّحْمَنِ الرَّحِيمِ

(وَمَا أُوتِيتُمْ مِنَ الْعِلْمِ إِلَّا قَلِيلًا)

صدق الله العظيم

(الإسراء: ٨٥)

وزارة التعليم العالي والبحث العلمي

جامعة بابل - كلية الهندسة

قسم الهندسة الميكانيكية

التحليل النظري والعملي للاستجابة العابرة لمنظومة تثليج صغيرة

رسالة

مقدمة إلى كلية الهندسة في جامعة بابل كجزء من متطلبات نيل درجة
الماجستير علوم في الهندسة الميكانيكية/ قدره

من قبل

زهرة حمود جلهام

بإشراف

د. عادل عباس الموسوي

Acknowledgement

The author wishes to express his deep gratitude and sincere thanks to Assist. Prof. Dr. Adil AL-moosawy whose pithy and cogent discussion, patient guidance and continued supervision made this work possible.

The great help and support of the author's colleagues, friends and family is highly appreciated especially that of Mr. Ali noumean, Dr. Saba Yasoup, Mr. Sahir Raqem, Mr. Mushtaq Fessal and from Baghdad university Miss. Lina Esmaeal for their assistance. Thanks are also due to the staff of the Air-conditioning laboratory for their assistance. Finally to my family, without their sincere effort and special care, this work would not have appeared at all.

Zehra H. Gelham

JAN. 2006

Dedication

To all of our Professors who labored and toiled, to teach and to instruct, to open our eyes, widen our horizon and to inspire us with awe of this stunning world.

To my mother and father who brought me in pain into this world with love never complaining.

To my husband without him this work would not have appeared.

To my dear son Yousif.

Zehra

خلاصة البحث

يتناول البحث دراسة التغيرات الفيزيائية التي تحدث لمائع الشغل في كل مكونة من مكونات وحدة تثلج تعمل بدورة تبريد انضغاطية واعتمدت الحالة غير المستقرة (*unsteady*) في هذه الدراسة. حيث تمت مناقشة عمليات الجريان وانتقال الحرارة مع وصف نظري للعمليات التي تحدث داخل مكونات المنظومة من اجل تطوير نموذج رياضي للمنظومة وتشمل الدراسة الأجزاء التالية: المبادل الحراري (المكثف والمبخر) وصمام الخنق والضاغط. إن النموذج الرياضي الذي تم عمله إلى المكثف و المبخر اعتمد على المعادلات الفيزيائية لتوازن الكتلة والطاقة في حالة الجريان غير المستقر بالاعتماد على تغير الزمن. أما في للضاغط وصمام الخنق فان العمليات اعتبرت مستقرة وذلك لأنها تحدث بسرعة اكبر من المبادل الحراري.

تمت الدراسة النظرية على أساس الجريان المتجانس في المكثف والمبخر وعلى اعتماد الحالة غير المستقرة. وتم عمل أنموذجين منفصلين باستخدام فرضيتين: الفرضية الأولى: هي طريقة السعات المجمعة (*Lumped*) وتم في هذه الطريقة توقع معدل التغيرات لدرجات الحرارة كتوزيع حقيقي للمسافات والزمن.

و الفرضية الثانية هي طريقة التوزيع (*Distributed*) لتوقع التغير الموقعي لدرجة الحرارة والمحتوي الحراري في كل نقطة كدالة للزمن.

هذين الأنموذجين أعطوا وصفا نظريا جيدا للظواهر الفيزيائية التي تحدث لمائع الشغل في كل مكونة من مكونات وحدة تثلج.

النتائج العملية تم إنجازها بشكل حقيقي على وحدة تثلج نموذجيه مختبريه إيطالية الصنع .

خلاصة البحث

تم إعداد برنامج حاسوبي لكل طريقة لحساب الاستجابة العابرة لوحدة تثلج انضغاطية مبردة بالهواء تعمل بمائع التثلج. $\mathcal{R}134a$

النتائج العملية تم مقارنتها مع النتائج النظرية للطريقتين وأعطت نتيجة جيدة ومقاربة.

Certificate

I certify that this thesis entitled "A theoretical and Experimental Analysis of Transient Operation of A Small Scale Refrigeration System", was prepared by Zehra Hamod Gelham under my direct supervision at Babylon University/College of Engineering as a partial requirement of the Master Of Science degree in Mechanical Engineering.

Assist. Prof. Dr. Adil AL-moosawy

ABSTRACT

An unsteady- state model of vapor compression refrigeration system is presented. Thermal and flow processes occurring in a small-scale refrigeration system have been discussed. A theoretical description of the processes in the system components has been proposed in order to develop a theoretical model of the entire system. The model for the condenser and evaporator are obtained from the physical equations for mass and energy balance. The dynamic of the compressor and the expansion valve are much faster than those of the heat exchanger and are therefore modeled as static devices.

Components model include the heat exchangers (condenser and evaporator) and expansion valve. For the condenser and evaporator mathematical model, two approaches for homogenous refrigerant are used. The first approach is the lumped model and the second is distributed model. The first model predicted the average parameters from an actual distribution in time and space, and the second model predicted the spatial variation of the temperature, enthalpy at each point as a function of time.

The two models have been tested for consistency in the theoretical description of the physical phenomena occurring in individual components of the theoretical model on the basis of quantitative laws and relations.

Experimental investigations are carried out on the laboratory scale system model RCT/EV.

The results obtained from the models prediction are in a good agreement with the experimental results.

The system approaches its final steady-state operating condition in a few minutes.

Results of air cooled condenser indicated that the temperature of the tube wall increases to a high value at the beginning of the two-phase region, while in the air cooled evaporator the temperature of the tube wall decreases at the outset of superheated region.

The conclusion and suggestion for future work are provided, in the area of dynamic refrigerator simulations,

Examination Committee Report

We certify that we have read the thesis entitled “ **A theoretical and Experimental Analysis of Transient Operation of A Small Scale Refrigeration System**”, and as examining committee, examined the student **Zehra Hamod Gelham** in its contents and what is related to it, and that in our opinion, it meets the standard of a thesis for the degree of Master of Science in Mechanical Engineering.

Signature:

Name: **Dr. Adil AL-moosawy**

Assist. Professor

(Supervisor)

Date: / / ٢٠٠٦

Signature:

Signature:

Name: **Dr. Abed- Alkareem Abed Al- Alwahab**

Assist. Professor

(Member)

Date: / / ٢٠٠٦

Name: **Dr.Majid H. Majeed**

Assist. Professor

(Member)

Date: / / ٢٠٠٦

Signature:

Name: **Dr.Haroun A. K. Shahad**

Assist. Professor

(Chairman)

Date: / / ٢٠٠٦

Signature:

Signature

Name: **Dr.Abd AL-Wahid. K. Rajih**

Dean of Engineering College

Date: / / ٢٠٠٦

Name: **Assist. Prof. Dr. Adil A. AL-Moosawy**

Head of Mechanical Engineering

Date: / / ٢٠٠٦

Thermodynamic and Thermo physical Refrigerant Equations.

A.1 Thermodynamic Equations:

A set of computer-based methods for calculating densities, vapor pressure, enthalpies, and entropies for refrigerants, R-11, R-12, R-13, R-13B1, R-14, R-22, R-113, R-114 and R-600 are developed by Chan & Haselend (1981), [1981, 1981, 1981].

The equations used are in British units. However, the developed property module presents results in SI units.

1- Equation of state:

$$\begin{aligned}
 & + \frac{A(2) + B(2)T + C(2)\{\mu \exp(-KT/Tc) + v/T^3\}}{(v-b)^2} + P = \frac{RT}{v-b} \\
 & \frac{A(3) + B(3)T + C(3)\exp(-KT/Tc)}{(v-b)^3} + \frac{A(4) + B(4)T + C(4)\{\mu \exp(-KT/Tc) + v/T^3\}}{(v-b)^4} + \\
 & \frac{A(5) + B(5)T + C(5)\exp(-KT/Tc)}{(v-b)^5} + \frac{A(6) + B(6)T + C(6)\exp(-KT/Tc)}{\exp(av) \cdot \{1 + c' \exp(av)\}} \quad (A.1)
 \end{aligned}$$

Where $A(2-6)$, $B(1-6)$, μ, ν, T_c, b, R, c' are constants defined in table A.1 & A.2 for R-12, R-134a.

2- Saturation vapor pressure:

$$\begin{aligned}
 \log_{10} P_{sat} = & AVP(1) + AVP(2)/T + AVP(3)\log_{10} T + AVP(4)T + \\
 & [AVP(5) \frac{(AVP(6) - T)}{T} \log_{10} (|AVP(6) - T|)] + \frac{AVP(7)}{T^2} + AVP(8)T^2 \quad (A.2)
 \end{aligned}$$

Where $AVP(1-8)$ are constants defined in tables A.1 and A.2 for R-12 and R-134a.

ϒ-Liquid density:

$$\rho_l = \frac{1}{v_l} = RL(1) + RL(2)\left(1 - \frac{T}{T_c}\right)^{\frac{1}{3}} + RL(3)\left(1 - \frac{T}{T_c}\right)^{\frac{2}{3}} + RL(4)\left(1 - \frac{T}{T_c}\right) + RL(5)\left(1 - \frac{T}{T_c}\right)^{\frac{4}{3}} + RL(5)\left(1 - \frac{T}{T_c}\right)^{\frac{5}{3}} + RL(6)\left(1 - \frac{T}{T_c}\right)^{\frac{1}{2}} + RL(7)\left(1 - \frac{T}{T_c}\right)^2 \quad (\text{A.}\zeta)$$

Where $RL(1-7)$ are constants defined in tables A\'.1 and A\'.ϒ for R-1ϒ and R-1ϒξa.

ξ. specific heat capacity of vapor at zero pressure:

$$(\text{A.}\xi) \quad C_v^0 = ACV(1) + ACV(2)T + ACV(3)T^2 + ACV(4)T^3 + ACV(5)/T^2$$

Where $ACV(1-5)$ are constants defined in tables A\'.1 and A\'.ϒ for R-1ϒ and R-1ϒξa.

ο. Derivation of enthalpy:

From the four basic thermodynamic equations, and Maxwell's relationships of a one component system, the differential enthalpy can be expressed as:

$$(\text{A.}\omicron) \quad dH = C_v^0 dT + d(Pv - [P - T(\partial P / \partial T)_v])dv$$

For a given reference temperature and pressure (T_{ref}, P_{ref}) , the enthalpy at T and P .

$$(\text{A.}\uparrow) \quad H_{(T,P)} = \int_{T_{ref}}^T C_v^0 dT + \int_{P_{ref}, v_{ref}}^{P,v} d(pv) - \int_{v_{ref}}^v \{P - T(\partial p / \partial T)_v\} dv + H(T_{ref}, P_{ref})$$

Each of these integral terms is treated separately.

$$\int_{T_{ref}}^T C_v^0 dT = ACV(1)T + \frac{1}{2} ACV(2)T^2 + \frac{1}{3} ACV(3)T^3 + \frac{1}{4} ACV(4)T^4 - ACV(5)/T - C_{H_1} \quad (\text{A.}\Upsilon)$$

Where C_{H_1} is a constant for the same expression with T_{ref} replacing T .

To evaluate the two pressure- volume integral terms, the partial differential term $(\partial P / \partial T)_v$ has to be evaluated from equation A.1, substituting the resulting equation with equation A.1 into $\{P - T(\partial p / \partial T)_v\}$ and integrating the two terms.

$$\begin{aligned}
 & + pv \int_{P_{ref}, v_{ref}}^{P, v} d(pv) - \int_{v_{ref}}^v \{P - T(\partial p / \partial T)_v\} dv = \\
 & \frac{A(2) + C(2)\{\mu(1 + KT / T_c) \exp(-KT / Tc) + 4v / T^3\}}{(v - b)} + \\
 & \frac{A(3) + C(3)\{\mu(1 + KT / T_c) \exp(-KT / Tc)\}}{2(v - b)^2} + \\
 & \frac{A(4) + C(4)\{\mu(1 + KT / T_c) \exp(-KT / Tc) + 4v / T^3\}}{3(v - b)^3} +
 \end{aligned}$$

(A.1)

$$\frac{A(5) + C(5)\{\mu(1 + KT / T_c) \exp(-KT / Tc)\}}{4(v - b)^4} - \left(\frac{A(6) + C(6)\{\mu(1 + KT / T_c) \exp(-KT / Tc)\}}{a} \right) \times$$

$$[(C' \ln\{C' + \exp(-av)\} - \exp(-av))] - C_{H_2}$$

is the same expression described by P_{ref}, v_{ref} and $T_{ref} \cdot C_{H_2}$

(A.1)

The enthalpy expression is then obtained from substitution of equations A.1 & A.1 in equation A.1.

1. derivation of entropy:

Using the same basic thermodynamic equations, the differential of entropy is given by;

$$(A.9) \quad dS = \frac{c_v^0}{T} dT + \left\{ \frac{\partial P}{\partial T} \right\}_v dv$$

The expression for entropy, at given T and T , with specified reference condition, is ;

$$(A.10) \quad S_{(T,P)} = \int_{T_{ref}}^T \frac{c_v^0}{T} dT + \int_{v_{ref}}^v \left\{ \frac{\partial P}{\partial T} \right\}_v dv + S_{ref}(T_{ref}, P_{ref})$$

Integrating the specific heat integral term;

$$\int_{T_{ref}}^T \frac{c_v^0}{T} dT = ACV(1) \ln(T) + ACV(2)T + \frac{1}{2} ACV(3)T^2 + \frac{1}{3} ACV(4)T^3 - ACV(5)/2T^2 - C_{s1}$$

(A.11)

The pressure-volume integral term becomes;

$$\frac{A(2) - C(2) \{ \mu K / T_c \exp(-KT / Tc) + 3v / T^4 \}}{(v-b)} - \int_{v_{ref}}^v \left\{ \frac{\partial P}{\partial T} \right\}_v dv = R \ln(v-b) -$$

$$- \frac{A(4) - C(4) \{ \mu K / T_c \exp(-KT / Tc) + 4v / T^4 \}}{3(v-b)^3} + \left(\frac{A(3) - C(3) \{ \mu K / T_c \exp(-KT / Tc) \}}{2(v-b)^2} \right)$$

$$\frac{A(6) - C(6) \{ \mu K / T_c \exp(-KT / Tc) \}}{a} \times$$

$$(A.12) \quad [(C' \ln\{C' + \exp(-av)\} - \exp(-av))] - C_{S2}$$

and C_{S2} are constants for a given T_{ref} and P_{ref} . $C_{S1,2}$

The entropy expression is obtained by substituting equations A.11 & A.12 into A.10.

A.13. latent heat of vaporization:

From Clapeyron-Clausius equation for a single component system;

$$(A.13) \left\{ \frac{dP}{dT} \right\}_{sat} = \frac{Hfg}{T(v - vl)}$$

The saturation vapor specific volume is obtained by solving equation A.1 numerically. The saturation liquid specific volume, vl is determined by equation A.3. The differential term $\left(\frac{dP}{dT}\right)$ has to be derived from the vapor pressure equation A.2.

$$\left\{ \frac{dP}{dT} \right\}_{sat} = 2.3026.P \left\{ -\frac{AVP(2)}{T^2} + \frac{AVP(3)}{2.3026.T} + AVP(4) - \frac{AVP(5)}{2.3026.T} \left\{ 1 + \frac{AVP(6)}{T} \cdot \ln(|AVP(6) - T|) \right\} - \frac{2 \cdot AVP(7)}{T^3} + 2 \cdot AVP(8) \cdot T \right\} \quad (A.14)$$

A.14. thermo physical equation:

The thermo physical equations are presented by ASHRAE, thermo physical properties of refrigerants, (1996), pp.7-11 & 31-30.

For R-12.

Viscosity-liquid:

For R-12.

For $170 \leq T \leq 250$ K;

$$(A.10) \mu = (\exp(-3.81728 + 681.713/T)) \times 10^{-3}$$

For $250 \leq T \leq 300$ K;

$$(A.11) \mu = (-2.3601 + 0.0149 \times T - 0.000025T^2) \times 10^{-3}$$

For R-123a.

$$(A.12) \mu = (\exp(-5.451893 + 1139.97226/T)) \times 10^{-3}$$

Viscosity-saturated vapor:

For R-12.

For $250 \leq T \leq 300$ K;

$$(A.13) \mu = (-0.16244 + 1.7545 \times 10^{-3}T - 5.9912 \times 10^{-6}T^2 + 6.9637 \times 10^{-9}T^3) \times 10^{-3}$$

For R-123a.

$$(A.14) \mu = (-0.16843 + 1.8192 \times 10^{-3}T - 6.21213 \times 10^{-6}T^2 + 7.22637 \times 10^{-9}T^3) \times 10^{-3}$$

Viscosity-gas:

For $200 \leq T \leq 300$ K;

$$(A.15) \mu = (T^{\frac{1}{2}} / (0.75309 + 188.969/T - 803.786/T^2)) \times 10^{-6}$$

Thermal conductivity-liquid:

For R-12.

For $18.5 \leq T \leq 38.5$ K;

$$(A.21) \quad k = 0.1893 - 3.7125 \times 10^{-4} T$$

For R-134a.

$$(A.22) \quad k = 0.23813329 - 5.222 \times 10^{-4} T$$

Thermal conductivity-saturated vapor:

For R-12.

For $-20 \leq T \leq 22$ K;

$$(A.23) \quad k = 1.7033 \times 10^{-3} + 1.6796 \times 10^{-5} T + 3.9063 \times 10^{-8} T^2$$

For R-134a.

$$(A.24) \quad k = -0.1252643 + 8.94909 \times 10^{-4} T$$

Thermal conductivity- gas:

For R-12.

For $18.5 \leq T \leq 38.5$ K;

$$(A.25) \quad k = (T^2 / (313.34095 + 296726.2841/T + 43405530.17/T^2))$$

For R-134a.

$$(A.26) k = -0.01252643 + 8.94909 \times 10^{-5} T$$

Specific heat-liquid:

For $190 \leq T \leq 300$ K;

For R-12.

$$C_p = (4.02967 \times 10^{-2} - 9.71208 \times 10^{-3} T + 4.07078 \times 10^{-5} T^2 + 6.25641 \times 10^{-8} T^3) \times 10^3 \quad (A.27)$$

For $300 \leq T \leq 380$ K;

$$C_p = (16.7169 + 1.83132 \times 10^{-1} T - 6.37059 \times 10^{-4} T^2 + 7.47156 \times 10^{-7} T^3) \times 10^3 \quad (A.28)$$

For R-134a.

$$(A.29) C_p = (C_{p1} + C_{p2} + C_{p3}) \times 10^3$$

$$(A.30) C_{p1} = 1.31969 + 0.00462678 T_r - 8.56489 \times 10^{-7} T_r^2 - 1.39255 \times 10^{-7} T_r^3$$

$$(A.31) C_{p2} = -9.648981 \times 10^{-10} T_r^4 + 3.16997 \times 10^{-10} T_r^5 - 2.69741 \times 10^{-15} T_r^6$$

$$(A.32) C_{p3} = -9.987458 \times 10^{-14} T_r^7 + 8.898 \times 10^{-16} T_r^7$$

$$T_r = (T - 273.15)$$

Specific heat- saturated vapor:

For $200 \leq T \leq 340$ K;

$$(A.33) C_p = (-4.17115 + 5.2195 \times 10^{-2} T - 1.97519 \times 10^{-4} T^2 + 2.59884 \times 10^{-7} T^3) \times 10^3$$

For $340 \leq T \leq 370$ K;

$$(A.34) C_p = (-2.29644 \times 10^3 + 1.94615 \times 10 T - 5.49968 \times 10^{-2} T^2 + 5.18519 \times 10^{-5} T^3) \times 10^3$$

Specific heat- gas:

For $100 \leq T \leq 1000$ K;

$$(A.35) C_p = (0.427182 + 9.38152 \times 10^{-4} T - 6.89715 \times 10^{-7} T^2 + 1.780066 \times 10^{-10} T^3) \times 10^3$$

CONTENTS

		Page
Chapter One: Introduction		
1.1	General	2
1.2	Refrigeration Cycle	3
1.3	Component of Vapor Compression Cycle	5
1.3.1	Compressor	5
1.3.2	Condenser	6
1.3.3	Evaporator	7
1.3.4	Expansion Valve	7
1.4	Methods of Analysis of Refrigeration Cycle	8
1.4.1	Steady State Model	8
1.4.2	Unsteady State Model	8
1.5	Scope of the Present Work	9
Chapter Two: Literature Survey		11
2.1	Introduction	12

۲.۲	Overview of the Literature	۱۳
Chapter Three: Mathematical Model		۲۲
۳.۱	Introduction	۲۳
۳.۲	Modeling Approaches	۲۴
۳.۳	Mathematical Analysis	۲۶
۳.۳.۱	Heat Exchanger; Condenser and Evaporator	۲۶
۳.۳.۱.۱	First Model (Lumped Model)	۲۶
۳.۳.۱.۱.۱	Model Assumption	۲۷
۳.۳.۱.۱.۲	Numerical Analysis and Solution Procedure	۲۹
۳.۳.۱.۲	Second Model (Distributed Model)	۳۰
۳.۳.۱.۲.۱	Model Assumption	۳۰
۳.۳.۱.۲.۲	Conservation Equation	۳۱
۳.۳.۱.۲.۳	Heat Transfer Coefficient for Refrigerant Side	۳۲
۳.۳.۱.۲.۴	Heat Transfer Coefficient for Air Side	۳۴
۳.۳.۱.۲.۵	Pressure Drop	۳۵
۳.۳.۱.۲.۶	Numerical Analysis	۴۹
۳.۳.۱.۲.۷	Solution Procedure	۴۰
۳.۳.۲	Expansion Valve	۴۱
۳.۴	Logic Diagram	۴۱

		Page
۳.۵	Subroutines used in the Computation of Simple Refrigeration Cycle	۴۲
Chapter Four : Experimental Work		۵۰
۴.۱	Introduction	۵۶
۴.۲	Test Rig Layout	۵۶
۴.۲.۱	Refrigeration Unit	۵۷
۴.۲.۲	Measuring Instrumentation	۵۸
۴.۳	Calibration of Measuring Instrumentation	۵۹
۴.۴	Test Procedure	۶۰
Chapter Five : Results and Discussion		۷۳
۵.۱	Introduction	۷۴
۵.۲	First Model (Lumped Model)	۷۴
۵.۳	Second Model (Distributed Model)	۷۵
Chapter Six : Conclusions and Suggestions for Future Work		۱۰۰

٦.١	Conclusions	١٠١
٦.٢	Suggestions for Future Work	١٠٢
	References	١٠٣
	Appendices	١١١
	Appendix A : Thermodynamic and Thermo physical Refrigerant Equations.	١١٢
	Appendix B : Thermo physical equation for air	١٢١
	Appendix C : Subroutines Listing	١٢٤

List of Tables

Table No.	Title	Page No.
٥-١	A Sample of Theoretical and Experimental Data in the Condenser and Evaporator using Lumped Model	٩٢
٥-٢	A Sample of Theoretical and Experimental Results for	٩٣

	Refrigerant Cycle using Lumped Model	
o-3	A Sample of Theoretical and Experimental Results in the Condenser using Distributed Model at time = 3. second	94
o-4	A Sample of Theoretical and Experimental Results in the Condenser using Distributed Model at time = 6. second	95
o-5	A Sample of Theoretical and Experimental Results in the Condenser using Distributed Model at time = 9. second	96
o-6	A Sample of Theoretical and Experimental Results in the Evaporator using Distributed Model at time = 6. second	97
o-7	A Sample of Theoretical and Experimental Results in the Evaporator using Distributed Model at time = 9. second	98
o-8	A Sample of Theoretical and Experimental Results in the Evaporator using Distributed Model at time = 12. second	99
A.1	Thermodynamic Equation Constant for R-12	119
A.2	Thermodynamic Equation Constant for R-134a	120

List of Figures

Fig. No.	Title	Page No.
၁-၁	Schematic of Typical Vapor Compression Refrigeration Cycle	၃
၁-၂	p-h Diagram of Vapor Compression Cycle	၄
၃-၁	Model of the Heat Exchanger- Condenser (Evaporator)	၂၇
၃-၂	Computational of Lumped Model	၃၀
၃-၃	Flow Chart of Unsteady State using Lumped Model	၄၀
၃-၄	Flow Chart of Condenser Tube Analysis using Distributed Model	၄၇
၃-၅	Flow Chart of Evaporator Tube Analysis using Distributed Model	၅၁
၄-၁	Schematic Diagram of Test Rig Layout	၆၂
၄-၂	Photographical Diagram of Test Rig Layout	၆၃
၄-၃	Cross Section of Airtight Compressor	၆၆
၄-၄	Heat Exchanger-Condenser (Evaporator)	၆၇
၄-၅	Thermostatic Expansion Valve	၆၈
၄-၆	Capillary Tubes	၆၈
၄-၇	Digital Thermometers	၆၉
၄-၈	Pressure Gauges	၇၀
၄-၉	Flow meter	၇၁
၄-၁၀	Calibration of digital thermometers	၇၂
၅-၁	Theoretical Temperature Distribution of condenser and evaporator using Lumped Model	၇၈
၅-၂	Condenser and Evaporator pressures	၇၈
၅-၃	Theoretical and experimental Temperature Distribution of condenser and evaporator using Lumped Model	၇၉
၅-၄	Response of System Energy using Lumped Model	၇၉
၅-၅	Spatial Temperature Distribution in the Condenser using Distributed model at Time ၃၀ Second	၈၀
၅-၆	Spatial Temperature Distribution in the Condenser using Distributed model at Different Time	၈၀
၅-၇	Spatial Temperature Distribution in the Condenser using Distributed model at Different Time	၈၁
၅-၈	Theoretical and Experimental Spatial Temperature Distribution of tube Wall in the Condenser using Distributed model	၈၁
၅-၉	Theoretical Spatial Temperature Distribution of tube Wall in the Condenser using Distributed model at different time	၈၂
Fig.	Title	Page

No.		No.
o_10	Theoretical Spatial Temperature Distribution of tube Wall in the Condenser using Distributed model at different time	82
o_11	Refrigerant Side Heat Transfer Coefficient in the condenser using Distributed Model at Time 20 Second	83
o_12	Refrigerant Side Heat Transfer Coefficient in the condenser using Distributed Model at Different Time	83
o_13	Refrigerant Side Heat Transfer Coefficient in the condenser using Distributed Model at Different Time	84
o_14	Spatial Enthalpy Distribution in the condenser using Distributed Model at Time 30 Second	84
o_15	Spatial Enthalpy Distribution in the condenser using Distributed Model at Different Time	85
o_16	Spatial Enthalpy Distribution in the condenser using Distributed Model at Different Time	85
o_17	Air Side Heat Transfer Coefficient in the condenser using Distributed Model at Time 20 Second	86
o_18	Air Side Heat Transfer Coefficient in the condenser using Distributed Model at Different Time	86
o_19	Condenser Pressure Drop using Distributed Model at Time 20 Second	87
o_20	Condenser Pressure Drop using Distributed Model at Different Time	87
o_21	Theoretical Spatial Temperature Distribution of Refrigerant in the Evaporator using distributed model at different time	88
o_22	Theoretical Spatial Temperature Distribution of tube Wall in the Evaporator using distributed model	88
o_23	Theoretical and Experimental Spatial Temperature Distribution of Tube Wall in the Evaporator using distributed model	89
o_24	Refrigerant Side Heat Transfer Coefficient in the Evaporator using Distributed Model at Different Time	89
o_25	Spatial Enthalpy Distribution in the Evaporator using Distributed Model at Different Time	90
o_26	Evaporator Pressure Drop using Distributed Model at Time 30 Second	90
o_27	Evaporator Pressure Drop using Distributed Model at Different Time	91

Nomenclature

Symbols	Description	Units
A	Cross section area	m^2
C_{ev}	Flow coefficient	-
C_p	Specific heat at constant pressure	J/kg. °C
C_v	Specific heat at constant volume	J/kg. °C
D_o	Outside diameter	m
d_i	Inside diameter	m
f	Friction factor	-
G	Mass flux	$kg/s.m^2$
$G_{r,l}$	Saturated refrigerant mass flux	$kg/s.m^2$
H_f	Fin height from root to tip	M
h	heat transfer coefficient	$W/m^2. °C$
H	Specific enthalpy	J/kg
K	Thermal conductivity	$W/m. °C$
M	Mass	kg
\dot{m}	Mass flow rate	kg/S
N	Speed	rev/s
p	Pressure	bar
Pr	prandtl number	-
Re	Reylonds number	-
S	Entropy	J/kg. °C

s	Distance between fins surface to surface	m
T	Temperature	°C
U	Overall heat transfer coefficient	W/m ² . °C
V	Volume	m ³
v	Specific volume	m ³ /kg
x _{tt}	Lockhart Martinelli parameter	-
x	Refrigerant Quality	-
T _f	Thickness of fin	m
z	Distance	m

Subscript	Description
in	Refrigerant inlet
out	Refrigerant outlet
t	Tube Wall
i	The index increases a long the x-axis indexes
a	Air
L	Liquid
sp	Single phase
tp	Two phase

<i>g</i>	Gas
<i>ev.</i>	Expansion valve
<i>tm</i>	Transaction region
<i>r</i>	Refrigerant
<i>ri</i>	Refrigerant inlet to a given element
<i>ro</i>	Refrigerant out let to a given element
<i>rl</i>	Refrigerant saturated liquid
<i>rg</i>	Refrigerant saturated vapor

Greek Symbol	Description	Units
μ	Dynamic viscosity	kg / m. s
ν	kinematics viscosity = $\frac{\mu}{\rho}$	m ² /s
ρ	Density	kg / m ³
ΔP	Pressure drop	bar
θ	Temperature difference	°C

INTRODUCTION

1.1. General.

Refrigeration in the engineering sense means the transfer of heat from a lower temperature region to a high temperature one. Devices that produce refrigeration are called refrigerators [1]. A refrigerator is designed to cool an enclosed space to a set temperature. Many refrigerators consist of two

compartments that are maintained at different temperature. The freezer compartment is usually kept at temperature of about $(-10) ^\circ\text{C}$, fresh food compartment at $(0-1) ^\circ\text{C}$. Most refrigerators have only one refrigeration cycle and therefore only one compressor. This cycle operates at the conditions of the lower temperature compartment, the freezer compartment. To cool the fresh food compartment, cold air is circulated from the freezer to the fresh food compartment [7]. In household refrigerators the temperature control in freeze chamber is carried out by means of a temperature controller performing an on-off control. The peculiar character of the refrigerating unit design (including a compressor, engine unit) and of the geometry of the refrigerating chambers and the temperature field required in them impose a necessity to control temperature in a special way.

Some properties of the system result from such a way of control, i.e.

- Temperature and pressure are selected, important places of the refrigerating unit are highly variable in time during the on off procedure.
- Heat exchange and flow processes of the medium in the refrigerating unit are unsteady.

It leads to an obvious conclusion that the analysis of energy of such a refrigerating unit, cannot be made if classical methods for refrigeration cycles in steady and quasi-steady states are used. The problems connected with the unit performance from the viewpoint of its design and actual operation, which are difficult to determine quantitatively and often also qualitatively, impose a certain procedure, which, in general, can be presented as a set of two-way activities:

Model tests that consist in a theoretical description of physical phenomena occurring in individual components of the theoretical system (model) on the basis of quantitative law and relations, and experimental investigation carried out on the actual system [۳].

۱.۲. Refrigeration cycle.

A vapor-compression refrigeration cycle typically consists of a compressor, a condenser, an expansion valve and an evaporator. This system shown schematically in figure (۱-۱).

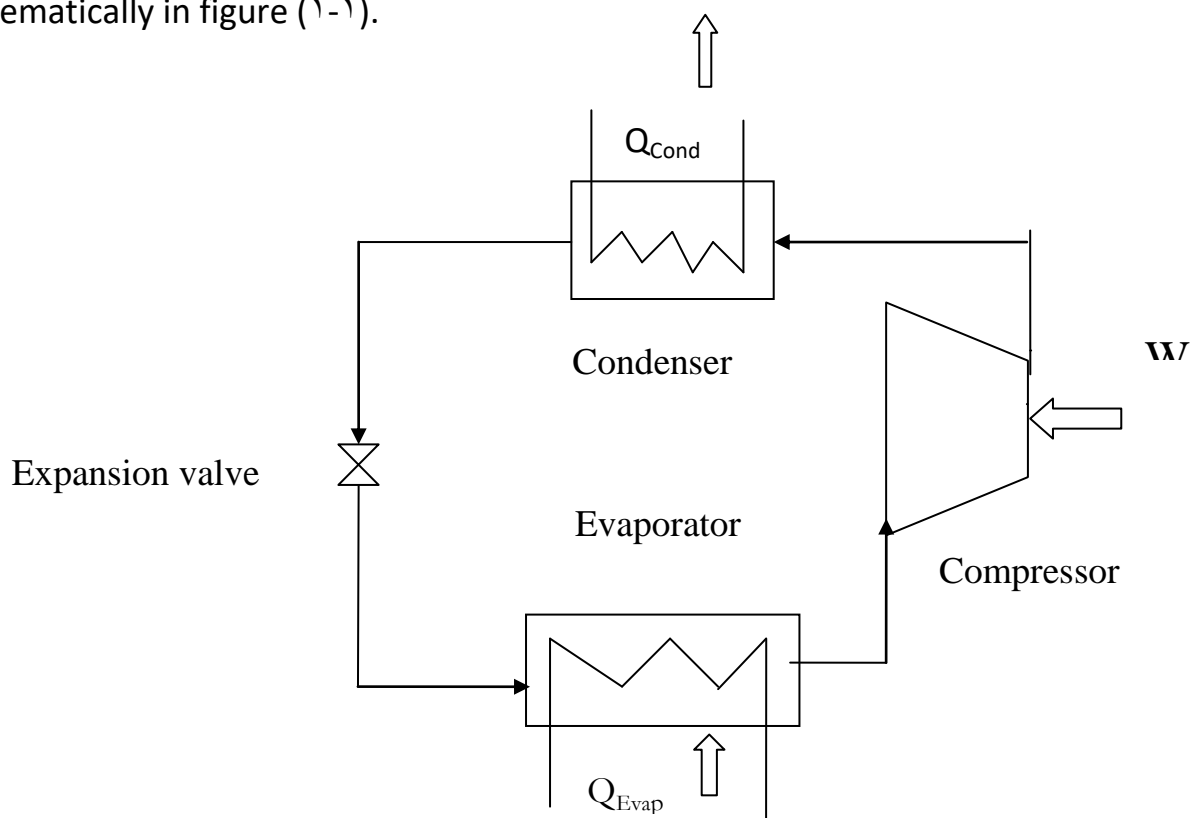
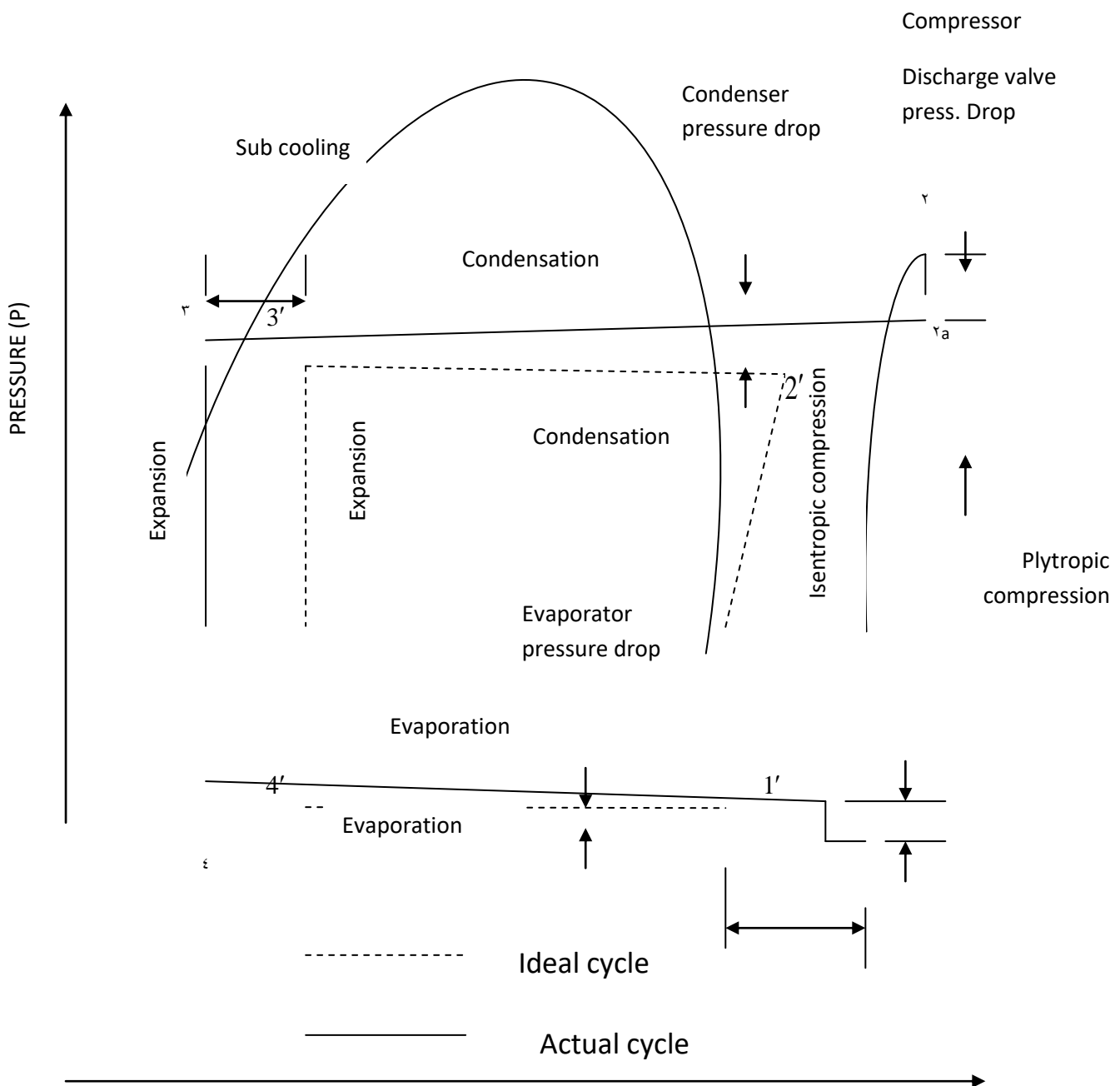


Figure (۱-۱) Schematic of typical vapor compression refrigeration cycle. Ref. [۳]

The vapor of the refrigerant is compressed to a higher pressure. This process requires mechanical work. In the condenser the refrigerant is cooled and then liquefied. The condenser is a heat exchanger behind or underneath the refrigerator that rejects heat to the ambient. The refrigerant then passes through an expansion device (usually a capillary tube) where the pressure is reduced.

The evaporator is located inside the freezer and/or fresh food compartment. The energy needed to evaporate the refrigerant is drawn from inside the refrigerator that is thereby cooled. Figure (1-2) is a pressure-enthalpy diagram showing both ideal and actual vapor-compression cycle. The numbers on this diagram show the state of the refrigerant as it enters and exits from the evaporator and condenser.



1" Compressor
 Super Suction valve press.
 Heating

ENTHALPY (h)

Figure (1-2) p-h diagram of vapor compression cycle. Ref. [4]

The processes, which comprise the standard vapor-compression cycle, are:

1-2 Reversible adiabatic compression from saturated vapor to the condenser pressure.

2-3 Rejection of heat at constant pressure, desuperheating, condensation.

3-4 Irreversible expansion at constant enthalpy from saturated liquid to the evaporator pressure.

4-1 Addition of heat at constant pressure in evaporation to saturated vapor.

An actual refrigeration cycle, deviates from a simple saturated cycle.

As shown in figure (1-2) the actual cycle has lower coefficient of performance, when compared with the simple saturated cycle. Pressure drop in the condenser and evaporator causes lower heat transfer with the ambient. Nonisentropic (polytropic) compression required more work and add extra heat to the refrigerant. The heat must be removed by extra heat rejection equipment; otherwise it will decrease the heat gain in the evaporator.

1.3 . Components of Vapor Compression System

The components of vapor compression system are:

i. **Compressor:** The compressor is one of the four essential components of the compression refrigeration system. There are two basic types of compressor: positive displacement and dynamic.

Positive displacement compressors increase the pressure of the refrigerant vapor by reducing the volume in the compressor chamber through work applied to the compressor's mechanism: reciprocating, rotary (rolling piston, rotary vane, single-screw, and twin-screw), scroll, and trochoidal. The reciprocating is by far the one most frequently used.

Dynamic compressors increase the pressure of refrigerant vapor by a continuous transfer of angular momentum from the rotating member to the vapor followed by the conversion of this momentum in to pressure rise. Centrifugal compressors which are used only on very large application, usually at least (100 tons) and above, work on this principle. The most widely used compressor is the halocarbon compressor, which is manufactured in three type of design: (a) open, (b) semi-hermetic or bolted hermetic, and (c) welded-shell hermetic [6]. The compressor is a central component of every refrigerator or freezer. It is the component that has to be supplied with electrical energy to

produce refrigerant mass flow to generate the desired cooling effect. An electrical motor converts the electrical energy into mechanical energy that is needed to operate the compressor. Most refrigerators use fixed speed compressor. These compressors do not operate at steady state but are started when the temperature in the freezer compartment rises above a set point. When the temperature in the freezer compartment reaches the low set point, the compressor shuts off and the refrigerant pressures in the system equalize. During the off cycle heat transfer occurs from the refrigerant to the surroundings and to air inside the refrigerator. The temperature and pressure under which the compressor operates vary considerably during this process [2].

ii. **Condenser:** The condenser is a heat transfer surface. Heat from hot refrigerant vapor pass through the walls of the condenser to the condensing medium. As a result of losing heat to the condensing medium, the refrigerant vapor is first cooled to saturation temperature and then condensed into the liquid state.

In the great majority of cases the condensing medium employed is either air or water, or a combination of both.

Condensers are of three general types:

(a) Air-cooled, (b) water-cooled, and (c) evaporative (air and water cooled).

Air-cooled condensers employ air as the condensing medium, whereas water-cooled condensers utilize water to condense the refrigerant. In both the air-cooled and water-cooled condensers, the heat given off by the condensing refrigerant increases the temperature of the air or water used as the condensing medium.

Evaporative condensers employ both air and water. Although there is some increase in temperature of the air passing through the condenser, the cooling of the refrigerant in the condenser results initially from the evaporation of the water from the surface of the condenser. The function of the air is to increase the rate of the evaporation by carrying away the water vapor, which results from the evaporating process.

iii- Evaporator: Any heat transfer surface in which a refrigerant is vaporized for the purpose of removing heat from the refrigerated space or material is called an evaporator [7]. The evaporators may be classified as forced convection type or free convection type depending upon whether the substance to be cooled is forced by pump or fan through the heat transfer surfaces of the evaporator, or it flows naturally by density difference of warmer and colder fluid. Some evaporators have refrigerant in the tubes and substance to be cooled surrounding the tubes, but, in other cases, the refrigerant is in the shell with substance to be cooled passing through the tubes. Evaporators also classified as flooded type and dry type depending upon whether liquid refrigerant covers all heat transfer surfaces or some portion is having gas being superheated. The evaporators with thermostatic expansion valve will have some portion of heat transfer surface where superheating is taking place and can be designated as dry evaporator; whereas evaporators with float valve will be flooded type.

iv. Expansion Device: The expansion device is a very important component of the vapor compression refrigerant system. Common expansion devices are [8]:

a. Capillary tube: - The capillary tube usually consists of an extremely small-bore tube from 0.5 mm to 2.5 mm of about 0.5 m to 9m long. It is usually used as an expansion and refrigerant controlling device for small refrigerating systems and household refrigerators. The process of refrigerant flows through

a capillary tube is a flash process, in which the state of the refrigerant changes from liquid to a vapor-liquid mixture [^].

b. Thermostatic expansion valve: This is the most popular and very efficient type of expansion device in use at present. The operation of thermo static valve is based on the principle of constant degree of super-heat for the evaporator exit. This ensures the evaporator completely filled with refrigerant irrespective of the load and also no liquid can spill over to the section line to the compressor. Because of its adaptability to load changes, it is especially suitable for variable load systems [^].

1.4. Methods of Analysis of Refrigeration Cycle.

Two approaches have been used to analyze refrigeration cycle: -

i. Steady- state model.

Steady state may be loosely defined as the point where electrical power input and cooling capacity remain essentially constant, provided that operation conditions are maintained constant. From a thermodynamic point of view, steady state occurs when flow properties at every point within the cycle remain constant (within experimental limits of courses) [^]. Many engineering devices operate essentially under the same conditions for long periods of time.

ii. Unsteady-state model.

Many processes of interest involve change the flow properties at every point within the cycle with time. Such processes are called unsteady-state or transient processes.

It is obvious that the state of the refrigerant in the system at start-up has a pronounced effect on the first minutes of operation in this critical period. As almost every refrigerating system operates under variable conditions, a pure

steady-state does not exist. Especially if controllers are fitted in the system. Investigations should not be limited only to steady state analysis, but should include non-steady-state or dynamic analysis. Unsteady-state modeling is a mathematical description of the system in the time domain.

Mass and energy accumulate or dissipate in the system are due to the difference between input and output of mass and energy to the system. The heat capacity of the tube and refrigerant act as a reservoir of heat energy. The two-phase flow takes place inside the evaporator and condenser tube is the reason for mass accumulation, thus the success of unsteady-state modeling depends to a large extent on the degree of understanding of the two-phase mechanism.

1.9. Scope of the Present Work

The scope of this research can be summarized in the following stages:

(i) Unsteady theoretical models description of the physical phenomena occurring in individual component, with particular attention given to the evaporator and condenser model on the basis of quantitative laws and relations. Since both condenser and evaporators are governed by the same physical, a generic heat exchanger model is developed that could be specified to operate as a condenser or as an evaporator at the time of system execution, and numerical procedures have been developed. Two computer programs have been developed. The first program depends on a simplified (initial) model of the condenser (evaporator). In this model, it has been assumed that the homogeneous refrigerant, of the thermodynamic properties which will correspond to average parameters from an actual distribution in time and space occurs in the whole inner volume of the condenser (evaporator). The second

program depends on the distributed model which uses node-to-node simulation; of the condenser (evaporator) to predict the unsteady state performance of the cycle. These details have been given within chapter three.

(ii) Experimental work which includes description of the test rig layout, the measuring instrumentation and the test procedure are given in chapter four.

(iii) The results of the theoretical analysis of the flow processes occurring in a small-scale refrigeration system is presented and compared with the experimental work in chapter five.

(iv) Conclusions and suggestions for further work are given in chapter six.

LITERATURE SURVEY

۲.۱. Introduction

In theory, the complete operation cycle of a refrigeration system can be characterized by two major time-regimes, namely transient and steady state. In steady state, the system input/output parameters are constant over time; transient operation is then, the non steady state. Typically, this case when the system is started-up and is approaching steady state, or when it is shutdown from a steady state, or when it is disturbed from its steady state. This

disturbance could be caused by either external changes in condition (such as load, ambient temperatures) or by feedback control. In either cases, the system attempts to move from one equilibrium state to another. Transient modeling is the predictive analysis of the system's operation during such condition. In practice, however, there exists a third time- regime in between the true steady state and transient perspectives, termed the 'quasi-steady state', in which the system transient responses are much faster than the transients of the inputs. This means that the system move quickly through a sequence of steady state, even while subjected to time varying conditions. This representation is useful when the time constants of the inputs and of the system are differing by order of magnitude. For such cases, steady-state modeling could be used to study transient behavior.

The process of building a system transient model consists primarily of building transient models of the individual components and then investigating them into a whole system. For the system model to truly represent actual behavior, each of the components must in themselves be accurate. This requires a sound understanding of the phenomena occurring in these components and the ability to mathematically represent these phenomena to the degree of the accuracy needed.

A pre-requisite for building a mathematical model is the identification of the scale of the transients of interest. The transients of a system could be categorized as small scale and large scale, based on the relative time-constants of the responses and their causes. Large-scale transients are caused by load

changes, start-up, shutdown, feedback control, etc and the responses are scaled on the same order-of-magnitude as the total cycle time. Small-scale transients are caused by (possibly random) fluctuations in conditions, e.g. compressor valve dynamics. The responses in this case are scaled on a much smaller time scale [10].

2.2. Overview of the Literature

Many mathematical models have been developed to simulate the thermal and flow processes occurring in vapor-compression system.

Wedekind and stoeker [11] described the transient response of horizontal evaporator. In this model the mixture transition point is calculated, which is useful for the preliminary evaluation of the performance of vapor simple cycle.

Refrigerant transport properties are not included in simulation.

Wedekind and stoeker [12] described also a theoretical model to predict the transient response of the mixture vapor transition point in horizontal evaporator flow. The study simulates a theoretical vapor compression cycle and departures from the theoretical cycle that occur in a heat pump and in a refrigerator when isenthalpic expansion process is assumed.

Marshall and James [13] described a dynamic analysis of a refrigeration system assuming a lumped model. The evaluation of the performance of the vapor compression refrigeration system is also described.

Wedekind et. al. [14] study transient behavior of two phase-flow dynamics in heat exchangers. In an attempt to simplify representation of two-phase flow, the model is built from a moving boundary formulation using a variable volume form of the volumetric mean void fraction over the two-phase region. A

significant achievement of this is that the complete two-phase region can be treated in adequate detail even in a lumped form, while avoiding the necessity of handling the transient form of the momentum equation.

Dhar and soedel [19] present one of the first models of a complete vapor compression refrigeration system. This model of a window air conditioner is built from first principles using a moving boundary approach in the heat exchangers. Two-phase refrigerant in the heat exchangers is treated as a coupled pair of lumps representing the liquid and vapor phases that exchange mass internally and heat externally. The model also accounts for refrigerant dissolution in the oil of the hermetic, reciprocating compressor. Despite using fairly simple representations, all major transients are well captured. The development focuses on the refrigerant side leaving the secondary fluid open to choice. This could arguably be used on the liquid chillers with the selection of a suitable compressor model.

Goldschmidt and hart [16] developed a lumped model for a refrigeration system with a view to study its seasonal performance when coupled to a mobile home whose heat losses were modeled in detail. The focus of this work being on the dynamics of the residence itself, and the air-to-air heat pump system itself is modeled by using an exponential fit to a steady state performance. The steady state performance of the heat pump is regressed from manufacturer's data and experimental measurements.

Chi and Didion's [17] model is among the few that works with the transient form of the momentum equation. Their model of an air-to-air heat pump system is built on a moving boundary lumped parameter formulation. The start-up transients when operating the model in cooling mode are analyzed. All the components, including the heat exchanger fans and the

motor shaft are included. The dynamic of all component are captured, including the momentum of air flowing across the heat exchangers and rotational inertial of the motor shaft. Dynamics of the valve however, are not considered significant.

Yasuda et. al. [14] built a complete system model, on lines similar to Dhar and soedel [10], except the condenser model is a shell-and-tube construction instead of air-cooled. The object of this model is to capture what are termed small transients. These include transients caused by feedback control and by instability triggered by poor valve setting. The purpose of this model being narrowly defined, broad assumption such as constant sub-cooling and uniform two-phase condition in the entire condenser, are found to work without serious consequence.

Mc Arthur [19] presents one of the earliest models that moves away from the lumped parameter approach toward a distribution formulation. This, along with McArthur and Grald [21] and Rasmuseen et. al. [22], constitute a body of work by using similar formulations for the system components. The space-time dependent conservation equations are simplified by assuming one dimensional flow in both heat exchangers. The two-phase region in the condenser is treated as a homogenous whereas in the evaporator the liquid and vapor phase are modeled separately. The Mc Arthur [19] work uses a simpler version of the heat exchanger formulation in that, the pressure response of the heat exchangers is de-coupled from the thermal response by the imposition of uniform flow velocities along the heat exchanger length. This yielded inaccurate mass distribution predictions and the issue is addressed in McArthur and Grald [21] where the mass balance is coupled to the energy balance and allowed to dictate the pressure response. In all of these, the heat

exchanger's discretizations were full implicit thereby allowing stable solutions for time steps up to 1 s. Rasmussen et. al. [22] build on this refined model, and include the compressor's prime mover, specifically an engine. The important thermal and inertial dynamics of the engine are modeled and coupled to the vapor compression heat pump system model. Murphy and Goldschmidt [20] developed simplified system models to study start-up and shutdown transients for an air-to-air system. In the start-up model, the dynamics dealt with are those of the capillary tube and the phenomenon of liquid backing up into the condenser during start up. The compressor is modeled from steady state measurements, and actual measurements of evaporator performance are used in place of an evaporator model. The condenser dynamics modeled are those of the refrigerant pressure response and the tube material. In the shutdown study, both the heat exchangers are modeled as tank containing two-phase refrigerant at different pressures to begin with, with air as a secondary fluid cooling or heating the coils by natural convection. The refrigerant is allowed to flow only through the capillary tube initially and subsequently also through a pressure equalization valve that opens shortly after shutdown begins. The liquid line is modeled in detail to capture the variation in refrigerant quality between entries and exit so as to ensure an accurate entry condition to the capillary tube, which predominantly controls the shutdown process.

Sami et. al. [23] used a lumped parameter approach to model the system components where the dynamic were relevant. Multiple component configurations are modeled including shell and tube condenser and evaporator, air-cooled condenser, direct expansion evaporator, capillary tube and thermostatic expansion valve. The model of the hermetically sealed reciprocating compressor is taken from yasuda et. al. [18] and enhanced by

including oil dissolution in the refrigerant. The heat exchangers are modeled by using a drift-flux model that consists of separating the vapor and liquid phases and coupling the mass and energy balances of the individual phases through the evaporation or condensation mass and energy exchange. Validation of the model is provided for the start-up performance of a liquid chiller. A unique case of a ground-coupled heat pump system was developed by Safemazandarani [10]. A transient model is constructed of the heat exchanger coupled to the ground and the system's response in cooling and heating modes is analyzed. As an improvement to the direct coupling of the heat exchanger with the ground, a proposal is analyzed in which a water bath is introduced between the heat exchanger and the ground. This proposal was found to require a smaller heat exchanger because of the improved heat transfer characteristics with the water.

Wang and Toubert [11] presented a distributed model that accounted for the two-phase evaporating flow by using a simplified void fraction propagation equation. The paper presents the derivation of the equations in unsteady-state modeling of air cooler. However, a constant evaporator temperature is assumed in the model. The pressure drop is only taken into account at the end of the two-phase region.

Nyers & Stoyan's [12] model of an evaporator is built on the moving boundary formulation using finite difference with each phase. This model has been used to predict the evaporator's behavior under step jump, exponential saturation, and periodic oscillation of the temperature and flow rate of the secondary fluid, compressor speed, condenser pressure, and throttle coefficient.

Vargas & Parise [13] studied the relative benefits of an alternative form of the closed-loop control method, based on a power-law, against the conventional on-off cycling. Their model is highly simplified, component level

lumped parameter formulation, used to highlight the improvements in cyclic energy efficiency when the proposed closed-loop control method is used.

Jia, Tso and Chia [27] presented distributed dynamic model that is applicable for the serpentine coil for dry-expansion evaporators. This model is capable of predicting distribution of the refrigerant temperature, tube wall temperature and air temperature, in both position and time domains. The model takes into account the refrigerant pressure drop inside the tube, as well as the moisture condensation on the airside. However, the two-phase evaporating flow inside the tube is simplified as homogeneous flow.

Sami and Comeau [28] and Sami and Dahmani [29] expanded on the model of Sami *et. al.* [23] to include finite differencing within the drift-flux model. This model was used to predict system performance. Sami and Comeau [29] work dealt with non-azeotropic refrigerant mixtures, specifically mixtures of R22-R113, R22-R113a and R22-R102a, while Sami and Dahmani [29] work dealt with HFC alternatives to R22, specifically, R407a, R410a and NARM40 (a blend of R22, R102a).

Ploug-Sorensen *et. al.* [30] constructed a model of a dynamic refrigerator, using the software package SINDA/FLUINT to demonstrate the capabilities of this package, which is used extensively in the aerospace industry. Using the domestic refrigerator as an example, the many features and mathematically infrastructure of the package are explained.

Xiandong he *et. al.* [31] developed a system model for a basic vapor compression refrigeration system, using the moving boundary lumped parameter formulation with the system mean void fraction method of Wedekind [32], for the purpose of studying the effect of multivariable feedback control. This model was then used to study a multi-input-multi-output (MIMO) control method developed by Xiandong he *et al* [31].

Williatzen *et. al.* [10] present a model for simulating the transient flow dynamics in a heat exchanger, in the form of a set of lumped parameter moving boundary formulation. The structure of the model allows for any physically possible combination of phases within the heat exchanger to be handled by an algorithm, which switches between the appropriate sets of equations. Pettit *et. al.* [11] applied this formulation to the case of an evaporator and studied the phenomena of the appearance and disappearance of phases-regions within the evaporator.

Rossi and Braun [12] developed a fast yet largely mechanistic model of a rooftop air conditioning unit. The importance of real time simulation is emphasized, and a smart automatic integration step-sizing algorithm is presented that robustly simulates start-up and on-off cycling. The system model is constructed using a fully finite-volume formulation of the mass and energy balances in the heat exchangers. Validation is presented using start up measurements of a 3-ton roof top unit.

Jing Xia *et. al.* [13] developed a separated flow model for an evaporator and studied the dynamics of the evaporator under variation of the compressor speed, condensing temperature, secondary fluid conditions and expansion valve opening.

Jakobsen *et. al.* [14] analyzed the relative accuracies of assuming homogenous flow and slip-flow patterns in the heat exchanger, and concluded that the homogenous flow model was an inadequate representation, which over-predicted the sensitivity of the evaporator. They recommend the use of the slip-flow model when the dynamics of the refrigerant are of interest.

Bin Farijan [15] presented an unsteady state model of vapor compression refrigerator. The components models include the condenser, evaporator, expansion valve and compressor. In predicting the transient response of the condenser and evaporator, the mathematical models are in distributed parameter

form and first-order differential equation are used to describe single and non-homogenous two-phase heat, mass and momentum transfer. Each point as function of time, for the condenser and evaporator, predicts the spatial variation of temperature, enthalpy, mass flow rate and density.

Svensson [30] was one of the few investigators to focus exclusively on liquid chillers. This model is constructed on a phase-wise lumped parameter formulation in the heat exchangers, which is adequate for the study of the dynamics of the system to load disturbances. These disturbances are introduced by step changes in the condenser side water flow rates.

Mechanistic, single stage and two stage centrifugal chiller models are presented in Wang and Wang [36]. A detailed model of the centrifugal compressor is developed from first principle, i.e. the momentum equation, the energy equation and the velocity triangles. All major losses namely hydrodynamic, mechanical and electrical are accounted for. Also incorporated is the inlet guide vane or pre-rotation vanes from of capacity control. The heat exchangers, however, are modeled in a highly simplified manner. Both are treated as single entity lumps with overall conductance and effectiveness correlated to the water flow rate and constructional parameters. The dynamics of the chiller are introduced in the form of lumped thermal capacitances to account for the refrigerant, heat exchanger body and secondary fluid (water in this case).

Browne and Bansal [37] developed and compared a simple physics based dynamic model with a dynamic neural network model of a screw chiller system.

The screw compressors are modeled as steady state devices incorporating capacity control in the form of varying the swept volume in the response to the error in the chilled water temperature. The dynamics of the system are in the

form of lumped elements for the heat exchangers material and the water. The refrigerant in the heat exchangers is treated quasi-statically.

Grace I.N. and Tassou S.A. [38] developed a simplified dynamic model of a liquid chiller consisting of a reciprocating compressor and shell-tube heat exchangers. The condenser has the refrigerant flowing in the shell and the evaporator has the refrigerant flowing in the tubes. The discretization and solution of the heat exchangers is developed by MacArthur and Gald [39]. The expansion device is a thermostatic valve with a sensing bulb. The expansion is modeled as isenthalpic. The superheated sensing bulb is modeled in detail by accounting for all the relevant heat transfer resistances and capacitances.

Shah, Alleyne and Rasmussen [40] presented the application of a multivariable adaptive control strategy to a typical automotive air conditioning system. First, an experimentally validated physical model for the air conditioning cycle is introduced. This is followed by the application of a multi-input multi-output (MIMO) parameter estimation algorithm to recursively identify an equivalent discrete time state space model of the system. A Linear Quadratic Regulator (LQR) design is implemented on the estimated model with the objectives of reference tracking and disturbance rejection. Simulation studies are performed to explore the idea of modulating the electronic expansion valve opening and airflow rate over the evaporator for controlling the efficiency and capacity of general automotive air conditioning unit

Maniam and Tumas [41] discussed the details of the air-conditioning module of the e-thermal. The basic components of automotive air conditioning system, evaporator, condenser, compressor, and expansion valve, are parametrically modeled in SINDA/FLUINT. For each component, physical characteristics and performance data is collected in form of component data

standards. This performance data is used to curve fit parameters that then reproduce the component performance. These component are then integrated together to form various A/C system configurations including orifice tube systems, thermal expansion valve (txv) system and dual evaporator systems. The A/C subsystem uses airflow rates, temperature, humidity's and compressor speed as inputs. The outputs include overall system energy balance, system C.O.P, refrigerant flow rates and system pressures. The A/C simulation mathematical model runs about three times faster to three times slower than real time. The model technique used is also capable of tracking the effect of system charge on the overall system performance.

It has been shown from the above researches reported here, that their mainly study concentrate on the dynamic modeling of refrigeration system. More progress is needed in a new technique to calculate the spatial and temporal temperature distribution for each component of refrigeration system. Therefore modern techniques (the explicit and implicit methods) are needed to give reliable solution of the transient heating phenomenon. Using these techniques in a numerical solutions to solve these equations which where constructed developed as models for simulating the thermal and flow processes occurring in vapor-compression system. Also in the experimental work using apparatus which was available in the laboratory.

۳.۱. Introduction

During transient operation all the components experience phenomena absent in steady state operation, due to non-uniformity of conditions within them. The refrigerant mass flow rate, in general, is continuously changing, causing changes in refrigerant distribution in the system components, inlet/outlet condition of the compressor and the operating point of the expansion device. Of the four major components in the vapor compression system, the transients in the heat exchangers are usually the slowest and have the largest

impact on transient performance. It is necessary to consider mass distribution within the heat exchangers as a function of the time and space and this requires transient mass balances to allow for local storage. Thermal capacitances of the heat exchanger bodies and the refrigerant have to be considered to account for local energy storage. When the secondary fluid is a liquid such as brine or water, the thermal inertial of this fluid also becomes a significant factor. To determine spatial and time variations of pressure within the heat exchangers, which is the driving potential for mass flow, the transient form of the momentum balance has to be used in some form. This is particularly complicated since it requires solution of Navier-Stokes equations for compressible flow.

In addition to predicting the important phenomena, the transient model should be fast enough to be practical. This requires the identification of suitable assumptions that can simplify the mathematical form without loss of relevant details. Efficient numerical techniques are also necessary to reduce the computation time, thereby allowing the model to run as close to real-time as is possible, while also constraining errors to acceptable limits.

In general, a transient model is a set of coupled space-time partial differential equations in mass, energy and momentum balances, which evolve to more manageable ordinary differential and algebraic equations when simplifying assumptions, are applied.

۳.۲. Modeling Approaches.

In general, a component may be modeled either from a known (manufactures) map of its performance or from basic engineering principles.

Use of component maps keeps the model close to known performance and makes it easier to keep track of the uncertainty. The flip side of using maps is that the model is applicable only within the range in which the map was generated, and extrapolation is risky. The first principle approach, on the other hand, is inherently more robust but also more expensive computationally. From the literature reviewed it was observed that the maps, when used, were adopted

only for the compressor. Invariably, the heat exchangers and expansion devices were modeled from first principles. Also, it was seen that the largest task in modeling a refrigeration system was, usually, the modeling of the heat exchangers.

For heat exchangers, a sub-classification of modeling techniques was found. These are the phase-dependent moving boundary method and the phase-independent finite difference methods. In the former approach, the heat exchanger is divided into sections of variable volume according to the state of the refrigerant, i.e. liquid, two phases or superheated. Since there is constant mass redistribution during transient operation, these volumes cannot be constant and it is necessary to track boundaries between adjacent volumes, which move within the heat exchanger. In the condenser this could lead to tracking two boundaries- one between the superheated vapor and the two phase regions, and the other between the two phase and the sub-cooled regions. Special attention needs to be given to situations when the phase boundary moves in or out of the heat exchanger, such as during large scale transients. For example, when a system is started up from a condition where it is in equilibrium with the ambient, the condenser typically contains only superheated vapor. Subsequently, as the compressor begins to lift the refrigerant from the evaporator to the condenser, condensation begins and the two- phase region develops. Further along in time, when sufficient refrigerant has been moved to the condenser, a sub-cooled, liquid region forms. In the finite difference approach, the governing conservation equations are approximated by a finite difference scheme that typically consists of dividing the heat exchangers into number of (possible constant volume) elements, and each element is defined with its own state properties. The formulation for any element is phase- independent and therefore identical in

all three phase. A third approach is to combine the moving boundary with finite differencing. This involves a phase-dependent finite differencing with elements whose volumes change over time with no element spanning phase boundaries.

Another sub-classification of modeling techniques is in the choice of a lumped versus distribution parameter method. The lumped parameter method is computationally simpler, since it results in a finite system of equations consisting of algebraic and 1st order, ordinary differential equations. However, the drawback is spatial detail is lost by averaging the state parameters over the complete control volume. The distributed method approach allows spatial variations to be monitored and is simpler in that the governing equations for all elements are identical, if the property relations can be suitably framed to be phase-independent. The level of spatial detail depends on the level of discretization. The trade-off with this approach is the much larger computational time required and greater attention to potential numerical instabilities.

In addition to the above classifications, the flow of two-phase refrigerant can be modeled either using a homogenous or a slip flow model. In the homogenous model the liquid and vapor phases are considered to be in thermal equilibrium and moving at the same velocity. In the slip flow model, the liquid and vapor phase velocities are different and the model needs to be built based on the nature of the flow, i.e. bubbly, slug, annular, etc. In such models, it is not necessary that the liquid and vapor phases would be in the thermal equilibrium at any section [10].

3.3. Mathematical Analysis

A theoretical model of the system must comprise component models, owing to which it will be possible to describe quantitatively, the physical phenomena corresponding to the effects occurring in component of the actual system [۳].

Thus, the theoretical model will consist of the models of a condenser an evaporator and brief description for the expansion valve and the compressor.

The purpose of the present work is to expand the body of heat mechanism solutions to include the cases of spatial and temporal distribution within the component system by two models distribution and lumped with different assumptions. A new technique of numerical solution (the explicit and implicit methods) used to give more realistic, unsteady-state description of the temperature profile induced by vapor compression refrigeration system.

۳.۳.۱. Heat exchanger condenser (evaporator).

The condenser and evaporator are wire and tube heat exchanger with air-cooled. The relevant physical laws applicable to the phenomenon of the refrigerant movement within the system are those that govern compressible fluid flow mechanics, and are, in the most general case, the law of the conservation of mass, energy and momentum.

Since both condenser and evaporator are governed by the same physical, a generic heat exchanger model is developed that could be specified to operate as a condenser or as an evaporator at the time of system execution [۴۶].

۳.۳.۱.۱. First model (lumped model).

A simplified model of the condenser (evaporator) is shown in figure (۳-۱). In this model, it is assumed that the homogenous refrigerant, has thermodynamic properties correspond to average parameters from an actual distribution in time and space occurs in the whole inner volume of condenser (evaporator).

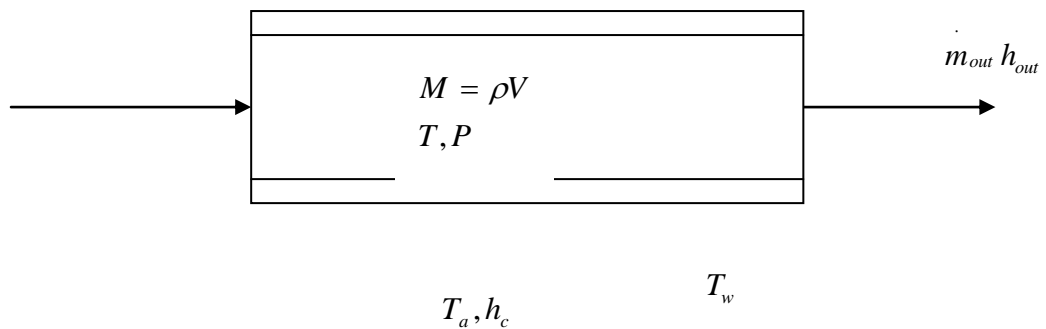


Figure (۳-۱) Model of the exchanger-condenser (evaporator). Ref. [۳]

۳.۳.۱.۱.۱. Model assumptions.

Owing to a complex design structure (from the view point of geometry) and physical processes occurring in a condenser (evaporator), which are difficult to describe mathematically, certain simplifications are assumed [۳].

- ۱- Refrigerant flow inside the tube is one dimensional along the tube axis.
- ۲- Pressure drop in the heat exchanger is negligible.
- ۳- In a cross section of the tube (of the condenser, evaporator), the refrigerant is homogenous (physical properties of the refrigerant are invariable in the cross section).
- ۴- Energy and mass transfer occurs only by convection.

To solve the equations for such a model, the boundary and initial conditions should be introduced; which is a difficult task due to the complicated geometrical structure of the exchanger (the shape, cooling fans

of the flow ducts). These conditions are most often a very simplified representation of the actual conditions.

The variation of the refrigerant mass in the inner volume of the heat exchanger (condenser, evaporator) is expressed by the relation:

.....(3.1)
$$dM = V.d\rho$$

The mass balance in the heat exchanger is written as:

.....(3.2)
$$\dot{m}_{in} - \dot{m}_{out} = \frac{dM}{dt} = V \frac{d\rho}{dt}$$

The heat balance for the heat exchanger is given by [3].

.....(3.3)
$$(\dot{m}_{in} H_{in} - \dot{m}_{out} H_{out})dt = cMdT + c_r M_r d\bar{T} + UA(T_w - T_a)$$

It can be assumed in the first approximation that:

$$T = \bar{T} = T_w$$

T - average temperature of the heat exchanger tube.

Assuming that

$$T - T_a = \theta$$

and T_a constant

.....(3.4)
$$\dot{m}_{in} H_{in} - \dot{m}_{out} H_{out} = (cM + c_r M_r) \frac{d\theta}{dt} + UA\theta$$

.....(3.5)
$$\dot{m}_{in} H_{in} - \dot{m}_{out} H_{out} = (cV\rho(T) + c_r M_r) \frac{d\theta}{dt} + UA\theta$$

where:

T_a - ambient temperature

T_w - wall temperature.

c - the specific heat of refrigerant at vapor phase.

M - mass of the refrigerant at vapor phase.

c_r - the specific heat of refrigerant at liquid phase.

M_r - mass of the refrigerant at liquid phase.

These parameters were represented the phase change happened in the condenser and evaporator.

Assuming that the heat resistance of the boundary layer on the refrigerant side and the heat resistance of the heat exchanger wall are negligible with respect to the heat resistance of the boundary layer on the airside, as:

$$\dot{m}_{in} H_{in} - \dot{m}_{out} H_{out} = (cV\rho(T) + c_r M_r) \frac{d\theta}{dt} + hA\theta \quad \dots\dots\dots(\text{3.7})$$

$$\dots\dots\dots(\text{3.7}) \quad h = 0.314 \frac{k_a}{D_o} \text{Re}^{0.68} \text{Pr}_{air}^{1/3} \left(\frac{H_f}{s}\right)^{-0.12} \left(\frac{T_f}{s}\right)^{-0.12}$$

Next, if we assume that the pressure pulsation of the refrigerant caused by the compressor operation is highly damped on its way towards the condenser, we can determine the mass flow rate at the condenser inlet, which is equal to the mass flow rate at the compressor outlet.

Equation (3.7) is non-linear, which is caused by the fact that the dependence of the variability of its parameters in the function of temperature and pressure are entangled in this equation (by compressing the refrigerant in the closed system). This variability is strongly influenced by the heat exchange taking place in the condenser. The refrigerant parameters at the condenser outlet depend on the refrigerant parameters in the condenser and the operation condition in the throttling element.

In the case of the evaporator, it is difficult to determine the inlet parameters as the correct determination of the throttling process in the

expansion device, which is strongly affected by variable thermodynamic properties of the refrigerant at the expansion device inlet, is very laborious [3].

3.3.1.1.2. Numerical and solution procedure.

By using finite difference method.

$$\dot{m}_{in} H_{in} - \dot{m}_{out} H_{out} = (cV\rho(T) + c_r M_r) \frac{d\theta}{dt} + hA\theta$$

$$(\dot{m}_{in} H_{in} - \dot{m}_{out} H_{out})^n = (cV\rho(T) + c_r M_r) \frac{\theta^{n+1} - \theta^n}{\Delta t} + hA\theta^n \quad \dots\dots\dots (3.8)$$

$$\theta^{n+1} = \frac{(\dot{m}_{in} H_{in} - \dot{m}_{out} H_{out})^n \Delta t}{(cV\rho(T) + c_r M_r)} + (1 - \frac{hA\Delta t}{(cV\rho(T) + c_r M_r)})\theta^n \quad \dots\dots\dots (3.9)$$

Equation (3.9) has fully explicit form defines the response of the average temperature occurs in the whole inner volume of the heat exchanger. In explicit formulation there is only one point at the (n+1) layer, and the temperature at that point which can be easily calculated from the values of the previous time layer (n) as shown in figure (3-2).

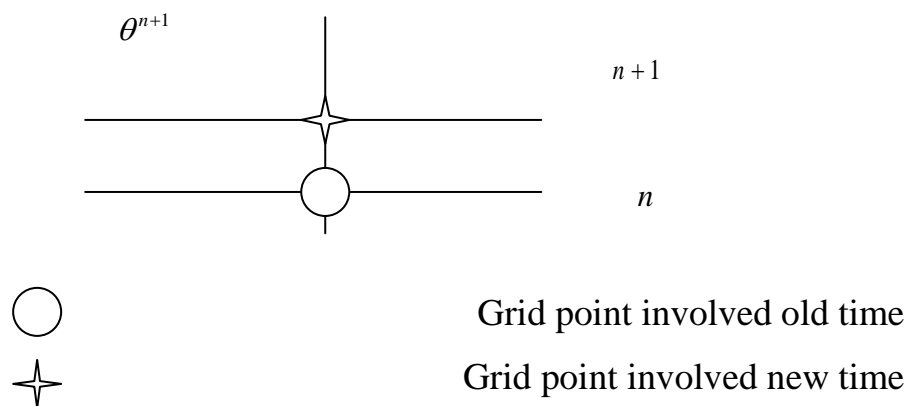


Figure (3-2) computational of lumped model

The initial conditions can be set to the saturated refrigerant vapor in the heat exchangers at a pressure equal to saturation pressure at the ambient temperature of the heat exchanger.

The boundary conditions applied are the refrigerant conditions at the tube coil of the heat exchanger. The inlet boundary conditions for the condenser are the compressor mass flow rate and the discharge enthalpy, where the exit boundary condition is the expansion valve mass flow rate. In the case of the evaporator, the inlet boundary conditions are the expansion valve mass flow rate and the enthalpy leaving the condenser, where the outlet boundary condition is the mass flow rate into the compressor.

The saturated refrigerant properties are calculated for the current pressure, at the beginning of each time step, then the field iterations continue with the newly calculated values of the properties, until the system reaches its steady-state condition.

3.3.1.2. Second Model (Distributed Model).

The distributed model allows spatial variations to be monitored and the governing equations for all the nodes are identical [10].

3.3.1.2.1. Model Assumptions:

Some of the common assumptions are [11 and 12]:

1)-The flow inside the tube is one dimensional along the tube axis.

ϒ-The two phase region of refrigerant is assumed to be a homogeneous mixture of liquid and vapor.

ϒ-The heat transfer coefficient is uniform on the air side.

ξ-The variation of refrigerant kinetic and potential energy is ignored.

⊖-The tube is so thin and the thermal conductivity of copper is so high, the conduction resistance in the radial direction is negligible.

⌒-Axial heat conduction in the tube wall is negligible.

ϒ.ϒ.⊖.⌒.⌒. Conservation Equation

By applying the conservation equations of mass and energy on the refrigerant and tube wall, the following basic equation can be obtained.

The mass conservation is represented by:

$$\dots\dots\dots (\text{ϒ.⊖.⊖}) \frac{d(\rho V)_i}{dt} = \dot{m}_{i-1} - \dot{m}_i$$

The energy conservation is given by:

$$\dots\dots\dots (\text{ϒ.⊖.⌒}) \frac{d(\rho V h)_i}{dt} = \dot{m}_{i-1} H_{i-1} - \dot{m}_i H_i - q_{r,i}$$

The rate of heat transfer is determined using the rate of equation:

$$\dots\dots\dots (\text{ϒ.⊖.⌒}) q_{r,i} = h_i A_i (T_{r,i} - T_{t,i})$$

The temperature of the tube is determined from an energy balance across the tube material in that node.

$$\dots\dots\dots (\text{ϒ.⊖.⌒}) M_t c_t \frac{dT_{t,i}}{dt} = q_{r,i} - q_{a,i}$$

The airside heat rate is determined as.

$$\dots\dots\dots (3.15) \quad q_{a,i} = h_o A_o (T_{t,i} - T_a)$$

3.3.1.2.3. Heat Transfer Coefficient for Refrigerant Side:

In heat exchanger the flow region can always be divided into two completely different regions: two phase and single-phase flow regions.

Most of the length of the heat exchanger tube passed by the refrigerant belongs to the two-phase flow region. In refrigerant system heat exchangers, the flow patterns in two- phase flow region are mostly annular flow [12].

Single- phase flow region occurs in superheated region and sub-cooled region in the condenser.

The refrigerant heat transfer coefficient depends on the phase of the refrigerant, however in two- phase; heat transfer is also depends on the direction of heat transfer, i.e., condensation or evaporation [1].

The heat transfer coefficient for condensation of R134a due to forced convection is given by Dobson [1] as:

$$\dots\dots\dots (3.15) \quad h_p = \frac{0.06003 \times Re_l^{0.8} \times Pr_l^{0.3} \times K_l}{D_l \times X_{tt}^{0.8}}$$

$$\dots\dots\dots (3.16) \quad X_{tt} = \left(\frac{\rho_g}{\rho_l}\right)^{0.5} \left(\frac{\mu_l}{\mu_g}\right)^{0.125} \left(\frac{1-x}{x}\right)^{0.875}$$

The two-phase heat transfer coefficients described above are used when the refrigerant quality is away from vapor and liquid state, the two-phase correlation cannot be applied where the quality is very low or very high.

Conventional single-phase heat transfer relationships for flow regimes in circular tubes are used for liquid and superheated vapor regions. For these region $0 \leq x \leq 0.1$ and $0.95 \leq x \leq 1$ the coefficient is computed by linear interpolation as follow [43].

For $0 \leq x \leq 0.1$

$$\dots\dots\dots (3.17) \frac{xh_p + (0.1 - x)h_{sp}}{0.1} h_p =$$

For $0.95 \leq x \leq 1$

$$\dots\dots\dots (3.18) \frac{(1 - x)h_p + (x - 0.95)h_{sp}}{0.05} h_p =$$

The heat transfer coefficient for evaporating process for vapor quality between 0.2 to 0.9 is obtained by using the Lockart- Martinelli parameter [44].

$$\dots\dots\dots (3.19) h_{pe} = c \left(\frac{1}{X_t} \right)^n h_l$$

$$\dots\dots\dots (3.20) \left(\frac{k_l}{Di} \right) \left(\frac{DiG}{\mu_l} \right)^{0.8} (Pr_l)^{0.4} h_l = 0.023$$

where c and n are constants depending on operation conditions. In horizontal pipes with commonly used refrigerants [45].

$$c = 3.4$$

$$n = 0.4$$

The transition region, according to Pierre's correlation should then be between an inlet quality of 0.9 and a leaving quality of 1.0. Thus, the

refrigerant heat transfer coefficient in this region is obtained by interpolating the two phase and superheated values. The following smooth interpolation function is used [20 and 21]:

$$\dots\dots(3.21) \quad h_m = h_{tp} \cdot \sin^2\left(\frac{\pi}{2}(1-\omega)\right) + h_{sp} \cdot \cos^2\left(\frac{\pi}{2}(1-\omega)\right)$$

Where $\omega = \frac{x - x_m}{1 - x_m}$ \dots\dots(3.22)

Where x_m = quality at the inlet to transition region.

The smooth interpolation function avoided abrupt changes in the heat transfer coefficient and is presumed to simulate actual conditions better than a linear interpolation function [20 and 21].

The single-phase refrigerant side heat transfer coefficient for $Re < 1000$ is computed using correlation given by Hiller and Glicksman [2] and utilized by Anand and Tree [22] in their steady state simulation. Its application is determined by the Reynolds number region and is given for each of the following flow regimes as;

1) Laminar flow, ($Re < 3500$)

$$\dots\dots(3.23) \quad h_{sp} = 1.1064 G_r c p_r Re^{-0.78992} Pr^{-2/3}$$

2) Transition flow, ($3500 \leq Re \leq 6000$)

$$\dots\dots(3.24) \quad h_{sp} = 3.5194 G_r c p_r Re^{-1.03804} Pr^{-2/3}$$

3) Turbulent flow, ($Re > 6000$)

$$\dots\dots(3.25) \quad h_{sp} = 0.018 G_r c p_r Re^{-0.1375} Pr^{-2/3}$$

Equation (3.25) is appropriate concerning the transition from laminar to turbulent flow. This region is defined approximately by $3500 < Re < 6000$ [22].

3.3.1.2.4. Heat Transfer Coefficient for Airside: Air is distributed uniform across a coil face area. A number of correlations have been published for heat transfer coefficient during flow across banks of finned tubes. The number and range of variables are so large that it would be surprising if a relatively simple correlation would be generally applicable. More complex correlations require correspondingly greater data sets with particular emphasis upon wide ranges of variables and multivariate interactions over these ranges, and the published data generally does not meet these criteria. Therefore, the published correlations must be used with a great care to ensure that they are applicable in the range of interest. One of the best-published correlations is due to [4].

$$\dots\dots\dots (3.26) h_o = 0.314 \frac{k_a}{D_o} \text{Re}^{0.68} \text{Pr}_{air}^{1/3} \left(\frac{H_f}{S}\right)^{-0.12} \left(\frac{T_f}{S}\right)^{-0.12}$$

Where $\text{Re} = \frac{\rho_{air} D_o v_{max}}{\mu_{air}}$

Is the maximum airside velocity going through the finned tube bank. v_{max}

3.3.1.2.5. Pressure drop:

(i) Two phase pressure drop: -

Pressure change in two-phase flow arises from three sources: -

- 1- Friction loss, which always causes a pressure decrease in the direction of flow. The pressure loss due to friction in a two-phase flow is generally much higher than in a comparable single-phase flow because of the roughness of the vapor-liquid interface. The pressure gradient due to friction depends upon local conditions, which change in a condensing flow. Therefore, the total pressure effects from friction depend upon the path of condensation.

- Ƴ- Momentum effects, which results from the change in the velocity, and hence kinetic energy, of the stream. The pressure change from this cause is negative (pressure loss) if the flow accelerates as in boiling and positive (pressure gain) if the flow decelerates, as is usual case in the condensation. The total effect on pressure from this cause depends only upon terminal conditions, though in some cases it may be necessary to calculate the local pressure gradient contributed by velocity changes.
- ƴ- Hydrostatic (gravitational) effects, resulting from changes in elevation of the fluid. The pressure source alone always decreases in an up ward direction and is zero in a horizontal tube. The local gradient depends upon the local density therefore; it is generally necessary to calculate contribution along the path of condensation [Ƴ 9].

In two-phase flow inside horizontal tubes, the pressure gradient is written as the sum of frictional and momentum terms. Neglecting the gravitational term, thus,

$$\dots\dots\dots(\text{Ƴ. Ƴ Ƴ}) \frac{dp}{dz} = \left(\frac{dp}{dz}\right)_f + \left(\frac{dp}{dz}\right)_m$$

A- Pressure drop through condensation: -

Friction pressure drop in the straight section of the tubes is calculated by the method of Lockhart and Martinelli [Ƴ 0].

$$\dots\dots\dots(\text{Ƴ. Ƴ 1}) f = 0.049 \text{Re}_{l,tp}^{-0.2}$$

Pressure drop is calculated by the following expression,

$$\dots\dots\dots(\text{Ƴ. Ƴ 9}) \Delta p_{tp} = \Phi_l^2 \Delta p_{x,l}$$

Where Φ_l is defined by:

$$\dots\dots(\text{3.30}) \quad \Phi_l = 1.467 - 0.51346 \times \ln(X_{tt}) + 0.048789 \times [\ln(X_{tt})]^2$$

Where $\Delta p_{x,l}$ is computed by:

$$\dots\dots(\text{3.31}) \quad \Delta p_{x,l} = 2fG_{r,l}^2 v_{ro} \frac{\Delta x}{D_i}$$

In the above expression, the mass velocity of the liquid, $G_{r,l}$, is given by:

$$G_{r,l} = (1 - x_m) \times G_r \quad \dots\dots(\text{3.32})$$

B- Pressure drop through evaporation:-

In homogenous flow, the two-phase mixture is treated as a single-component flow. Wallis [10] suggested the following equation to determine the friction pressure drop:

$$\dots\dots(\text{3.33}) \quad \Delta P_{fr,tp} = \frac{2 \cdot f \cdot G_r^2 \cdot (x_e \cdot v_{rg} + (1 - x_e)v_{rl}) \Delta X}{D_i}$$

Where x_e = elemental (mean) quality

$$\dots\dots(\text{3.34}) \quad f = 0.079 \times \left(\frac{1}{\text{Re}_r}\right)^{0.25}$$

$$\text{And } \text{Re}_r = \frac{G_r \times D_i}{\mu_r} \quad \dots\dots(\text{3.35})$$

The acceleration pressure drop is obtained by considering the one dimensional momentum equation. The pressure drop due to flow acceleration can be calculated by the following equation:

$$\dots\dots(\text{3.36}) \quad \Delta p_{acc} = G_r^2 \cdot (v_{ro} - v_{ri})$$

Which is applicable for single and two phase flow [ξ° and ξ٦].

(ii) single-phase pressure drop:

A- For vapor region in smooth tubes, the following is applicable;

١-Frictional pressure drop is calculated by the Fanning equation with the Fanning factor:

$$\Delta p_{r,sp} = f G_r^2 (v_{ro} + v_{ri}) \frac{\Delta x}{D_i} \dots\dots\dots(\text{٣.٣٧})$$

$$f = 0.046 \times \text{Re}^{-0.2} \dots\dots\dots(\text{٣.٣٨})$$

٢-Pressure drop due to momentum change is calculated by equation (٣. ٣٩).

٣-Gravity pressure drop is very small and may be neglected in actual heat exchangers.

Thus the total pressure drop can be calculated by summing up, as:

$$\dots\dots\dots(\text{٣.٤٠}) \quad \Delta p_{Total} = G_r^2 \left\{ f \frac{\Delta x}{D_i} (v_{ro} + v_{ri}) + (v_{ro} - v_{ri}) \right\}$$

B- For liquid phase in smooth tubes, using the normal incompressible flow relation:

$$\dots\dots\dots(\text{٣.٤١}) \quad \Delta p_{r,l} = 2 f G_r^2 v_{rl} \frac{\Delta x}{D_i} = \Delta p_{Total}$$

Where v_{rl} = liquid refrigerant specific volume, (m^٣/kg)

(iii) Return bend pressure drop: -

Pierre [10 and 11] divided the total flow resistance, or pressure drop, in return bend into two parts. The first is caused by the turning of the flow, and the second is caused by friction only. It is here assumed that the vapor quality is constant, in other words, no heat transfer takes place in the return bend.

$$\dots\dots\dots(3.12) \Delta p_{Total} = \Delta p_{Turning} + \Delta p_{fr}$$

$$\dots\dots\dots(3.13) \Delta p_{Turning} = Z_t \cdot G_r^2 \cdot \frac{v_{rb}}{2}$$

$$\dots\dots\dots(3.14) \Delta p_{fr} = Z_f \cdot G_r^2 \cdot \frac{v_{rb}}{2}$$

Where

: Specific volume at the vapor quality present in the return bend. v_{rb}

: the turning flow resistance factor. Z_t

: the friction resistance factor. Z_f

From single phase flow it is known that the effect of D/d (ratio between the bend diameter (D) and the tube diameter (d)) on Z_t is fairly small in the investigated range and this is also the case for two phase flow.

Thus, Z_t can be calculated as function of quality only eliminating the effect of D/d [10 and 11].

$$\dots\dots\dots(3.15) Z_t = 1.3021x^4 - 5.2662x^3 + 3.941x^2 - 0.0761x + 0.6996$$

For Z_f the following relation was derived from Pierre [10 and 11]:

$$\dots\dots\dots(3.16) Z_f = -9 \cdot 10^{-5} (D/d)^2 + 0.0483(D/d) + 0.0037$$

3.3.1.2.6. Numerical solution: -

Solution of the above mathematical model is a difficult task. Numerical methods give the possibility of getting an approximate solution. The governing differential equations have to be solved by finite difference method.

$$\frac{d(\rho V)_i}{dt} = m_{i-1} - m_i$$

$$\dots\dots\dots (\text{3.47}) \frac{d(\rho)_i}{dt} = m_{i-1} - m_i \quad i \quad V$$

$$\dots\dots\dots (\text{3.48}) \frac{(\rho_i^{n+1} - \rho_i^n)}{\Delta t} = (m_{i-1} - m_i)^{n+1} \quad i \quad V$$

$$\dots\dots\dots (\text{3.49}) \frac{\rho_i^n}{\Delta t} + (m_{i-1} - m_i)^{n+1} \quad i \quad V \quad \rho_i^{n+1} =$$

$$\dots\dots\dots (\text{3.50}) m_i^{n+1} = V_i \frac{(\rho_i^{n+1} - \rho_j^n)}{\Delta t} + m_{i-1}^{n+1}$$

The energy equation:

$$\dots\dots\dots (\text{3.51}) \frac{d(\rho V H)_i}{dt} = m_{i-1} H_{i-1} - m_i H_i - q_{r,i}$$

$$\dots\dots\dots (\text{3.52}) \frac{d(\rho H)_i}{dt} = m_{i-1} H_{i-1} - m_i H_i - q_{r,i} \quad i \quad V$$

$$\dots\dots\dots (\text{3.53}) \frac{(\rho H^{n+1} - \rho H^n)_i}{\Delta t} = (m_{i-1} H_{i-1} - m_i H_i)^{n+1} - q_{r,i} \quad i \quad V$$

$$= V \quad i \quad \frac{\rho H^n}{\Delta t} + (m_{i-1} H_{i-1} - m_i H_i)^{n+1} - q_{r,i} \quad \dots\dots\dots (\text{3.54}) \quad \rho H^{n+1}$$

Multiply equation (3.56) by H^{n+1} and subtracted from equation (3.60) to give:

$$\dots\dots\dots (3.56) \quad \frac{\rho i^n H_i^n + h_i A_i (T_{r,i} - T_{t,i}) \frac{\Delta t}{V_i} + m_{i-1} H_{i-1}^n \frac{\Delta t}{V_i}}{\rho i^n + m_{i-1} \frac{\Delta t}{V_i}} H_i^{n+1} =$$

For heat exchanger tube wall.

$$\dots\dots\dots (3.57) \quad M_{t,i} c p_t \frac{dT_{t,i}}{dt} = q_{r,i} - q_{a,i}$$

$$\dots\dots\dots (3.58) \quad M_{t,i} c p_t \frac{(T_{t,i}^{n+1} - T_{t,i}^n)}{\Delta t} = h_i A_i (T_{r,i} - T_{t,i}) - h_o A_o (T_{t,i} - T_a)$$

$$\dots\dots\dots (3.59) \quad \frac{h_o A_o T_a^{n+1} + h_i A_i T_i^{n+1} + T_i^n \frac{M_{t,i} C p_t}{\Delta t}}{\frac{M_{t,i} C p_t}{\Delta t} + h_o A_o + h_i A_i} T_{t,i}^{n+1} =$$

It has been considered for approximation purposes, that the grid spacing in both time and distance domains is equal. The index (i) will be used for indicating the points along the length of the heat exchangers and the index (n) will be used for indicating the points over the time layers. Notice that the temperature values in the time layer (n) are known, and that we search for the temperature values at the time (n+1). The partial derivative with respect to time is approximated by forward-difference scheme.

3.3.1.2.7. Solution procedure:

Equations (3.50), (3.56) and (3.59) are a set of fully-implicit equations defining the response of the ith nodes of the refrigerant and heat exchanger wall. The refrigerant passage of each heat exchanger is treated as node-by-node simulation.

In order to simplify the calculation the effect of piping between the heat exchanger and the next refrigerator component is neglected.

The above equations require a set of initial and boundary conditions. The initial conditions are set to the saturated refrigerant vapor in the heat exchangers at a pressure equal to the saturation pressure at the surrounding air temperature.

The boundary conditions applied are the refrigerant conditions at the tube coil and air conditions onto the heat exchangers coil. For refrigerant, the inlet boundary conditions for the condenser are the compressor mass flow rate and the discharge enthalpy, where the exit boundary condition is the expansion valve mass flow rate. For the evaporator, the inlet boundary conditions are the expansion valve mass flow rate and the enthalpy leaving the condenser, where the outlet boundary condition is the mass flow rate in to the compressor.

Air is distributed uniformly across a coil face area, thus each node is exposed to a fixed air flow rate.

At the beginning of each time step, the saturated refrigerant properties are calculated for the current pressure.

Sweeping the length of the heat exchanger from node i to node $i + 1$, equations (3.50 and 3.56) are solved in an alternative fashion to compute \dot{m}_i^{n+1} and H_i^{n+1} . The spatially dependent parameters the heat transfer coefficients and pressure drops are calculated during this sweep.

Employing equation (3.64) to find the heat exchanger piping wall temperature is solved, then the field iterations continue with the newly calculated values of the properties. This completes the calculations for one time step.

3.3.2. Expansion valve.

flow through the system. The expansion valve is used to control refrigerant Under normal condition the thermo-static expansion valve open or closed to maintain a fixed super heated vapor existing the evaporator [°³]. The expansion valve is modeled as a fixed orifice.

The standard orifice equation is used to calculate the mass flow rate through the valve [°]: -

$$m_{EV} = C_{EV} A_{EV} (2\rho_l \Delta P_{EV})^{0.5} \dots\dots\dots (3.60)$$

3.4. Logic Diagram

The present work is comprised of two main simulation programs:

1. The lumped model program, which predicts the average temporal parameters in the components of vapor compression refrigeration system with reciprocating compressor and air cooled condenser and evaporator.
2. The distributed model program, which predicts the spatial and temporal variation of the parameters in the same vapor compression refrigeration system.

The simulation programs are written in Fortran Power Station language. These programs are designed under XP environment for Pentium IV. The component subroutines can be tied together in a logical manner to simulate the refrigerant transient response of on-cycle.

In dynamic analysis, output from one component commonly constitutes input to the neighboring component and vice versa.

The computer program starts with initial condition values, the simulations are performed for the evaporator and condenser, which are divided into individual nodes, using a time step of 30 seconds.

In the two computer program the simulation time is initially set to be zero. The subroutine for expansion valve model is called to solve equation (3.60).

In the lumped model program the subroutine of the condenser is called with which equation (3.9) is solved. While in the distributed model the subroutine of the refrigerant side is called with which equations (3.50)-(3.56) are solved. Then the subroutine for the tube wall is called where equation (3.59) is solved.

For stability, the Newton-Raphson iteration algorithm is employed to solve this set of equations.

Meanwhile, the auxiliary subroutines, for the thermodynamic properties of refrigerant and air, the heat transfer coefficient of the refrigerant side and air side as well as the pressure drops are called (see appendices, A, B and C). The computational loop is repeated until the steady-state condition is reached.

3.5. Subroutines used in the Computation of Simple Refrigeration Cycle

Originally subroutines of these models were developed and presented by [50,56 and 57] in Fortran language, to enable specific volume, vapor pressure, liquid density, latent heat of vaporization, enthalpy and entropy to be calculated for different refrigerants.

The following list are subroutines developed by [50,56 and 57].

1. Sub CYENS :

- Calculates refrigerant pressure from equation of state, using equation A.1.

- Input variables : v, T

- Output variable : P

2. Sub CYSOV :

- Solving equation of state for refrigerant specific volume, utilizing equation A.1 in an iterative calculation program with a maximum of 100 iteration and a tolerance of 0.000001 bar.

- Input variables : T, P

- Output variable : v

γ. Sub CYVAP :

- Calculates saturated vapor pressure for a given temperature, using equation A.2.

-Input variables : T

- Output variable : saturated refrigerant pressure (P_{sat})

ξ. Sub CYLAH :

- Calculates refrigerant liquid specific volume and latent heat of vaporization, using equations A.3, A.4 and A.5

- Input variables : T, P, v

- Output variable : v_{rl}, H_{fg}

ο. Sub CYHH :

- Calculates refrigerant enthalpy, using equations A.6-A.8

- Input variables : T, P, v

-Parameters : C_{H1}, C_{H2} , reference enthalpy (H_{ref})

- Output variable : h

¶. Sub CYSS :

- Calculates refrigerant entropy, using equations A.11-A.12

- Input variables : T, P, v

- Parameters : C_{S1}, C_{S2} , reference entropy (S_{ref})

- Output variable : refrigerant entropy (S)

the following subroutines are develop by[¶^]:

∇. Sub SYTEM :

- Calculates refrigerant saturation temperature at a given pressure

- Input variables : P

- Output variable : saturation temperature (T_{sat})

∧. Sub SYPH :

- Calculates refrigerant temperature and specific volume at a given enthalpy

- Input variables : P, h

- Output variable : saturation temperature T, v

¶. Sub RSPHTC :

- Calculates refrigerant side single phase heat transfer coefficient using equations (3.23)-(3.25)

- Input variables : T, G_r, d_i, x

- Output variable : h_{sp} (RSPHTC)

10. Sub RTPHTC :

- Calculates refrigerant side two phase heat transfer coefficient using equation (3.10)

- Input variables : T, G_r, d_i, x

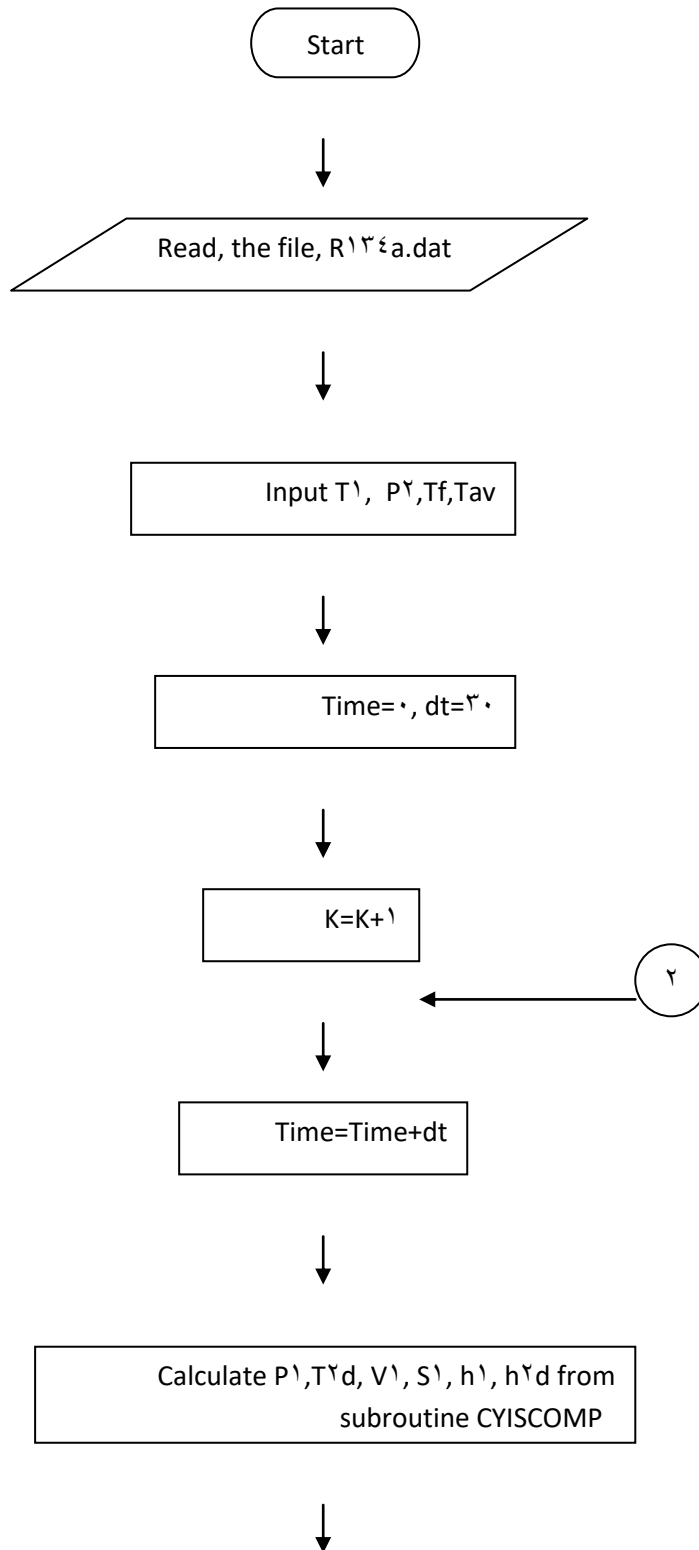
- Output variable : h_{tp} (RTPHTC)

11. Sub ASHTC :

- Calculates air side heat transfer coefficient using equation (3.26)

- Input variables : T_f, d_o

- Output variable : h_o (ASHTC)



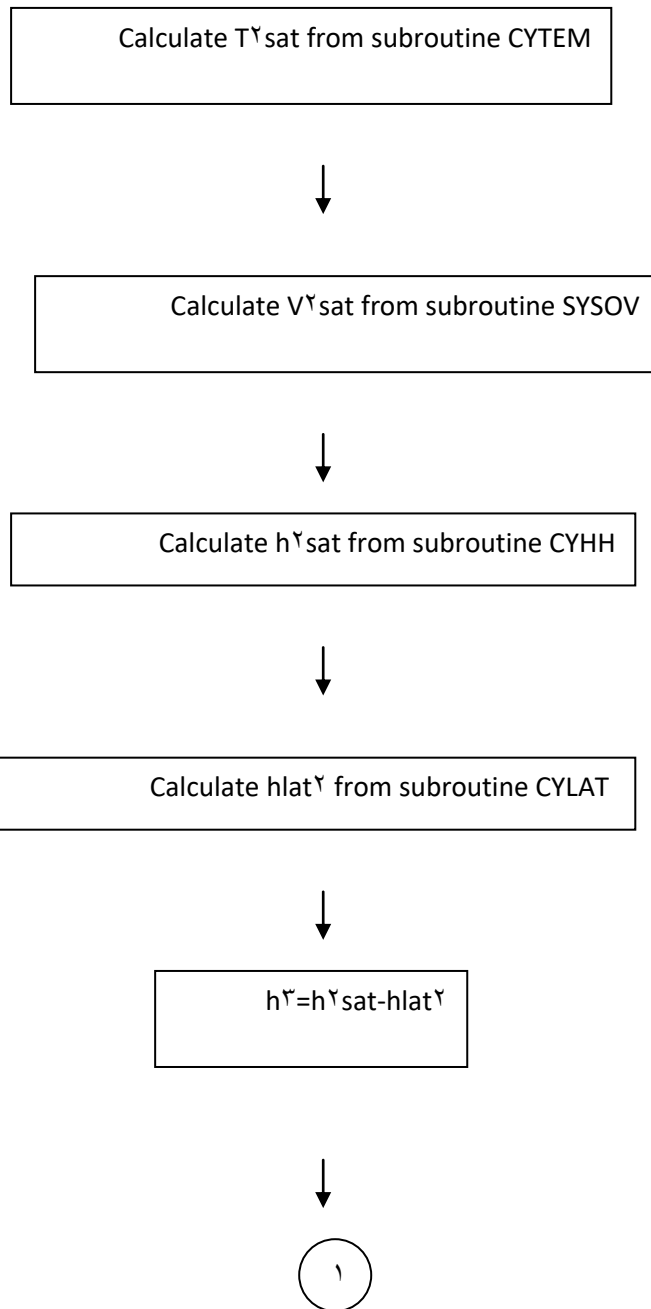


Figure (3- 3) Flowchart of unsteady state refrigerator using lumped model



$$h^{\xi} = h^{\tau} : CW = h^{\tau} d - h^{\lambda} : RE = h^{\lambda} - h^{\xi}$$



Calculate m_{ev} from subroutine CYEVM



Calculate m_{com} from subroutine CYCOM



Calculate V_{av} from subroutine CYSV



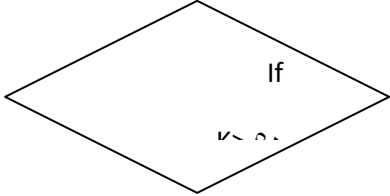
$$THETA = Tav - Tf$$



Calculate THETA from equation (7-1)



$$Tav = THETA + Tf$$



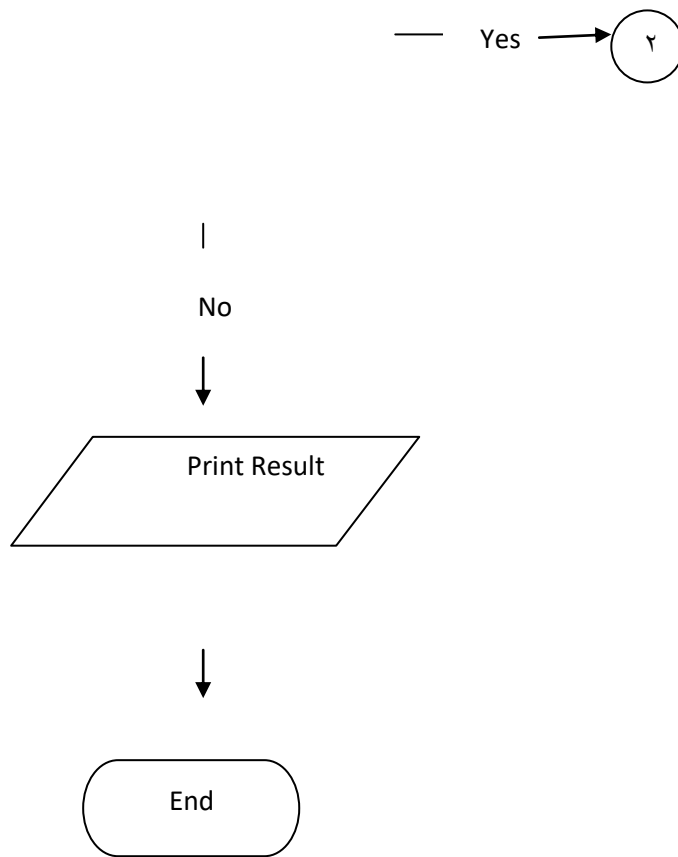


Figure (۳- ۳) continued

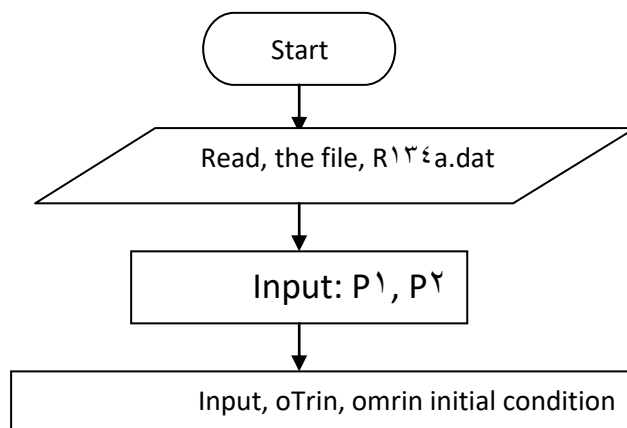
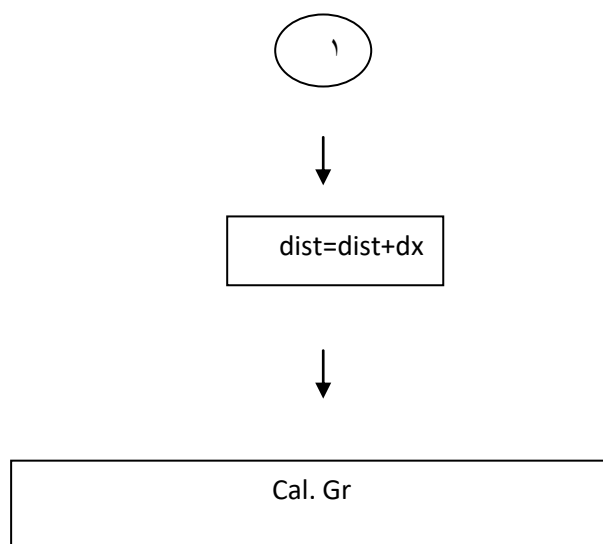
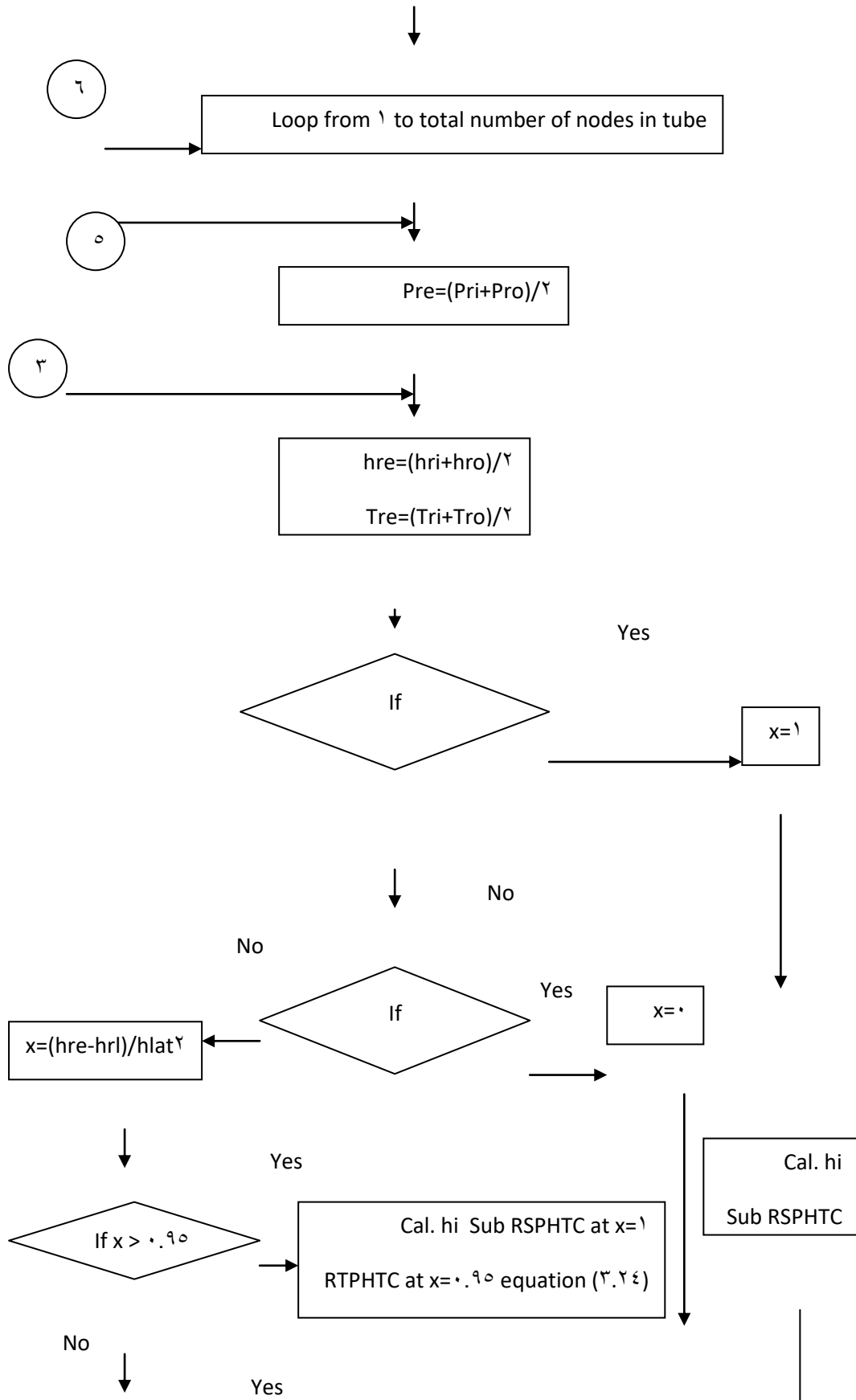
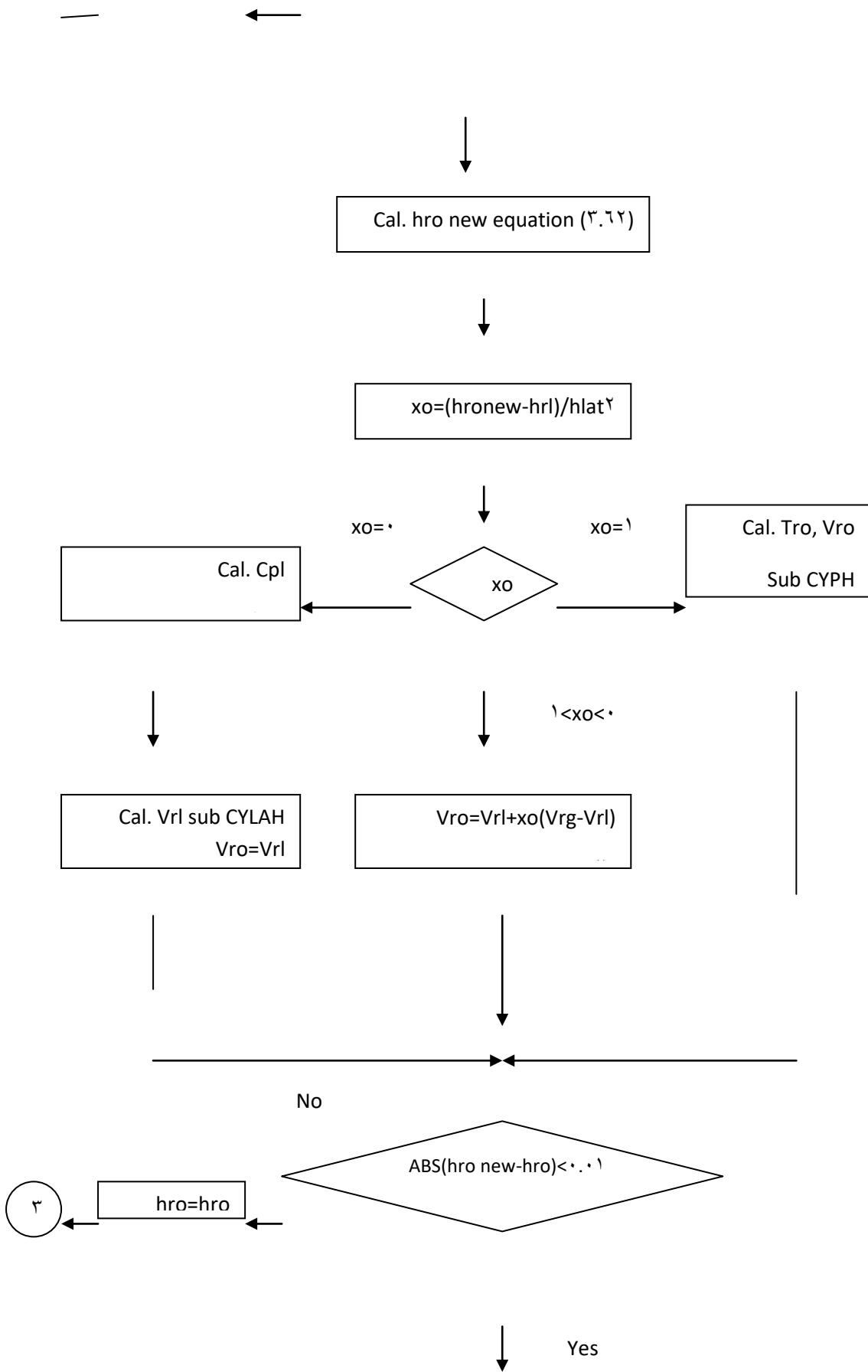


Figure (3-ε) Flowchart of condenser tube analysis using distributed model







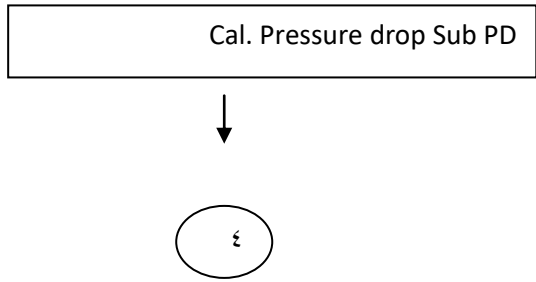
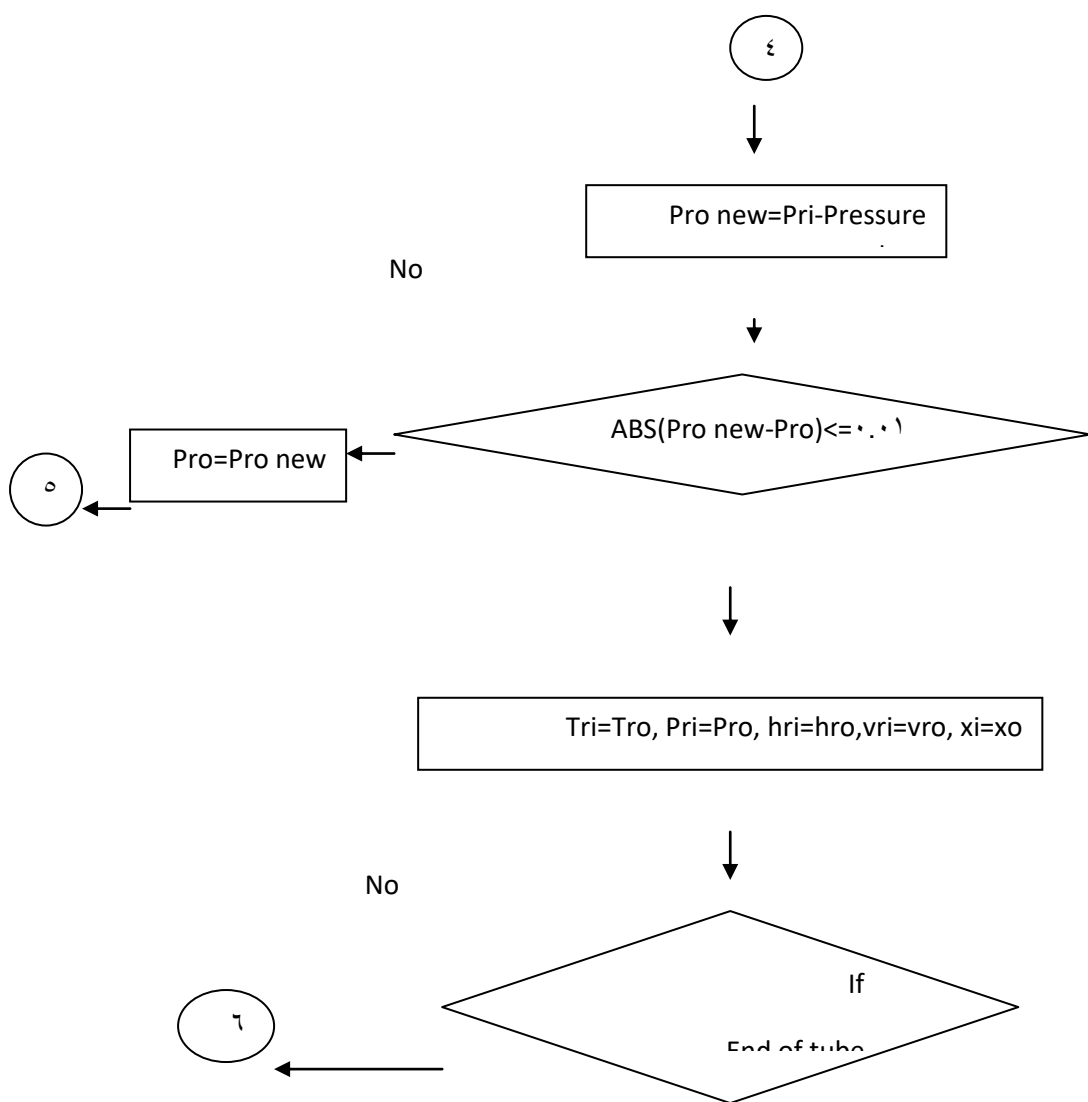


Figure (ξ-ξ) continued



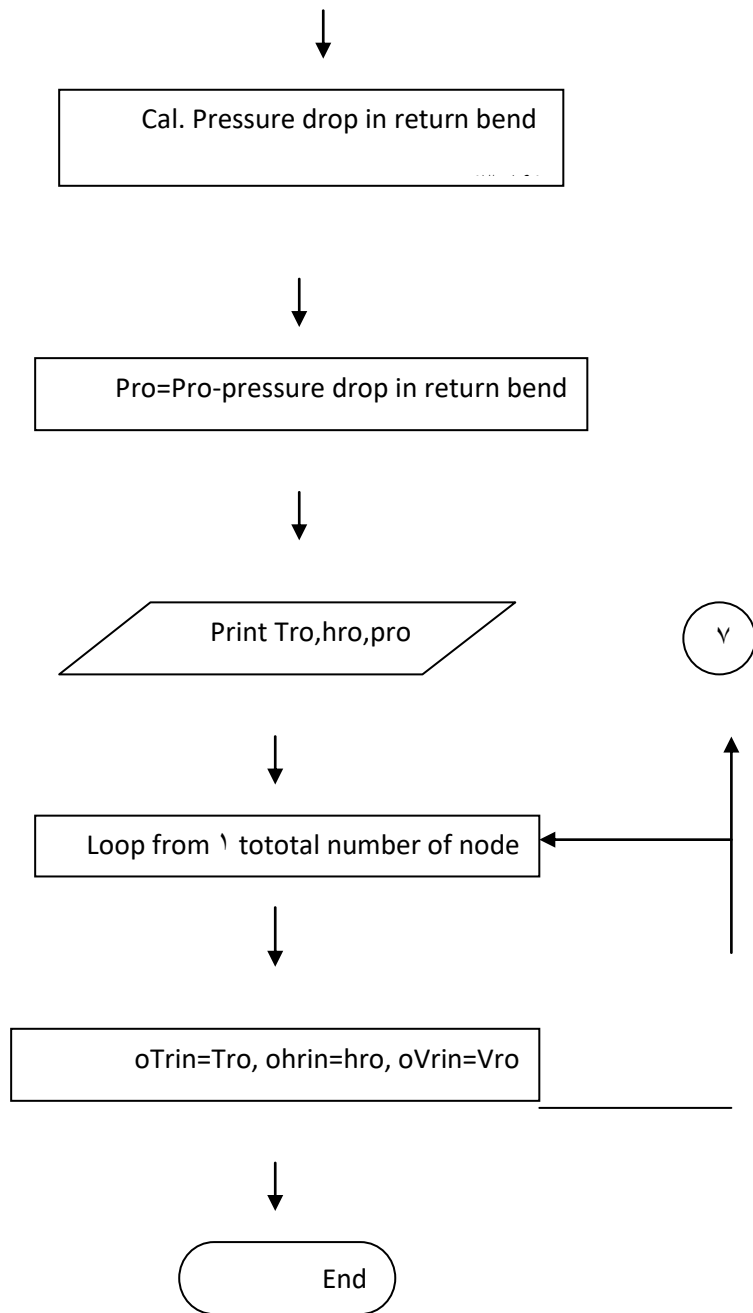
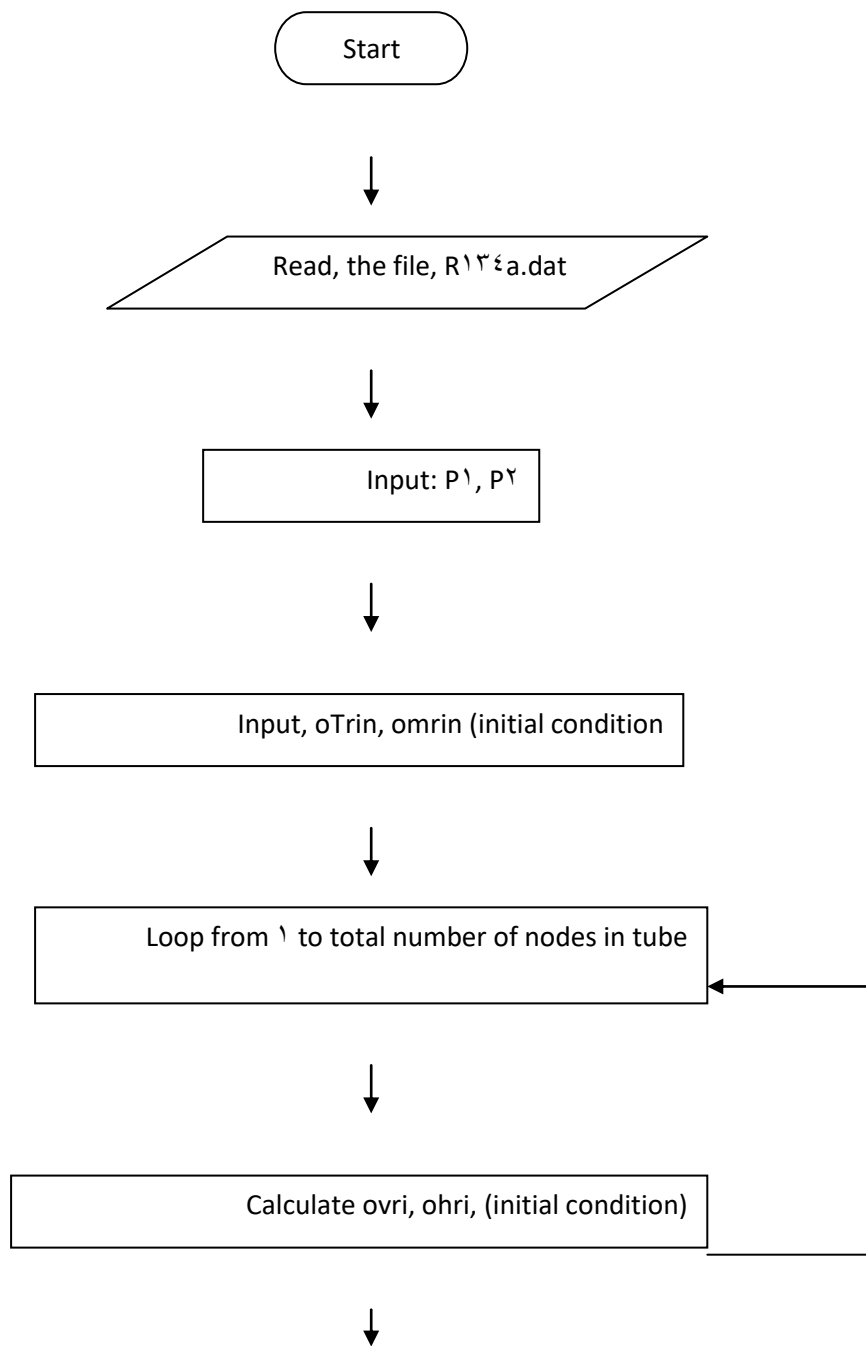


Figure (γ-ξ) continued



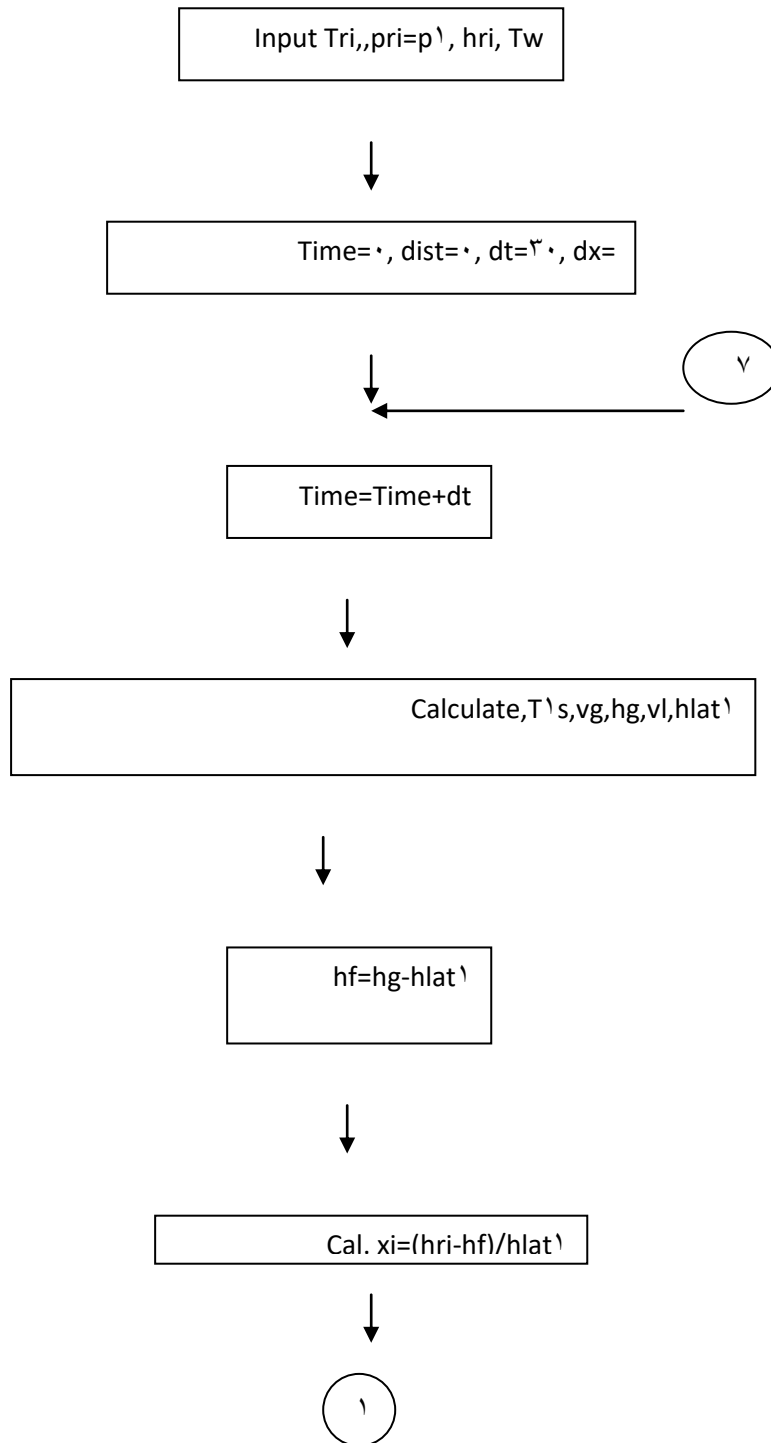
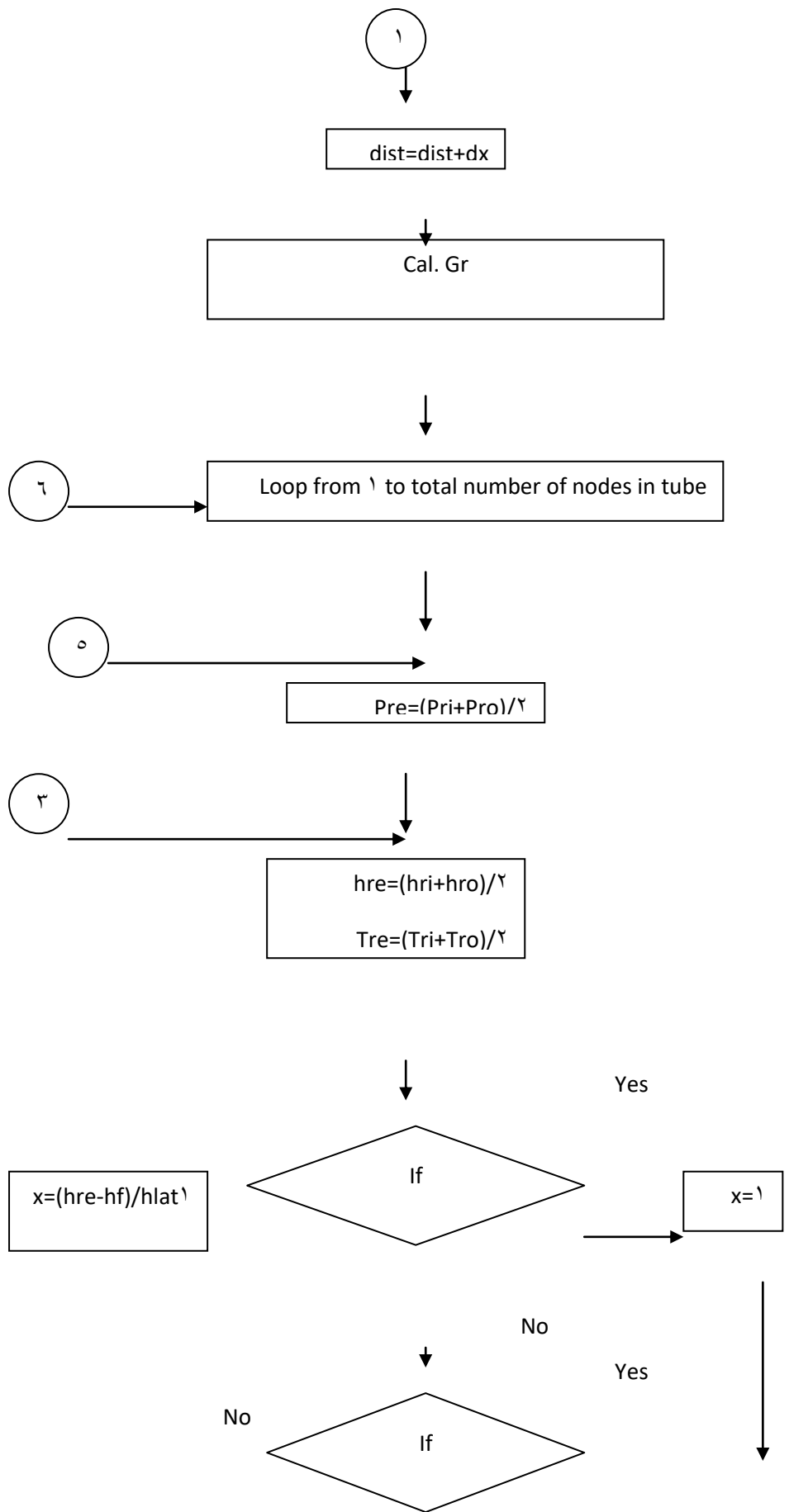


Figure (3-9) Flowchart of evaporator tube analysis using distributed model



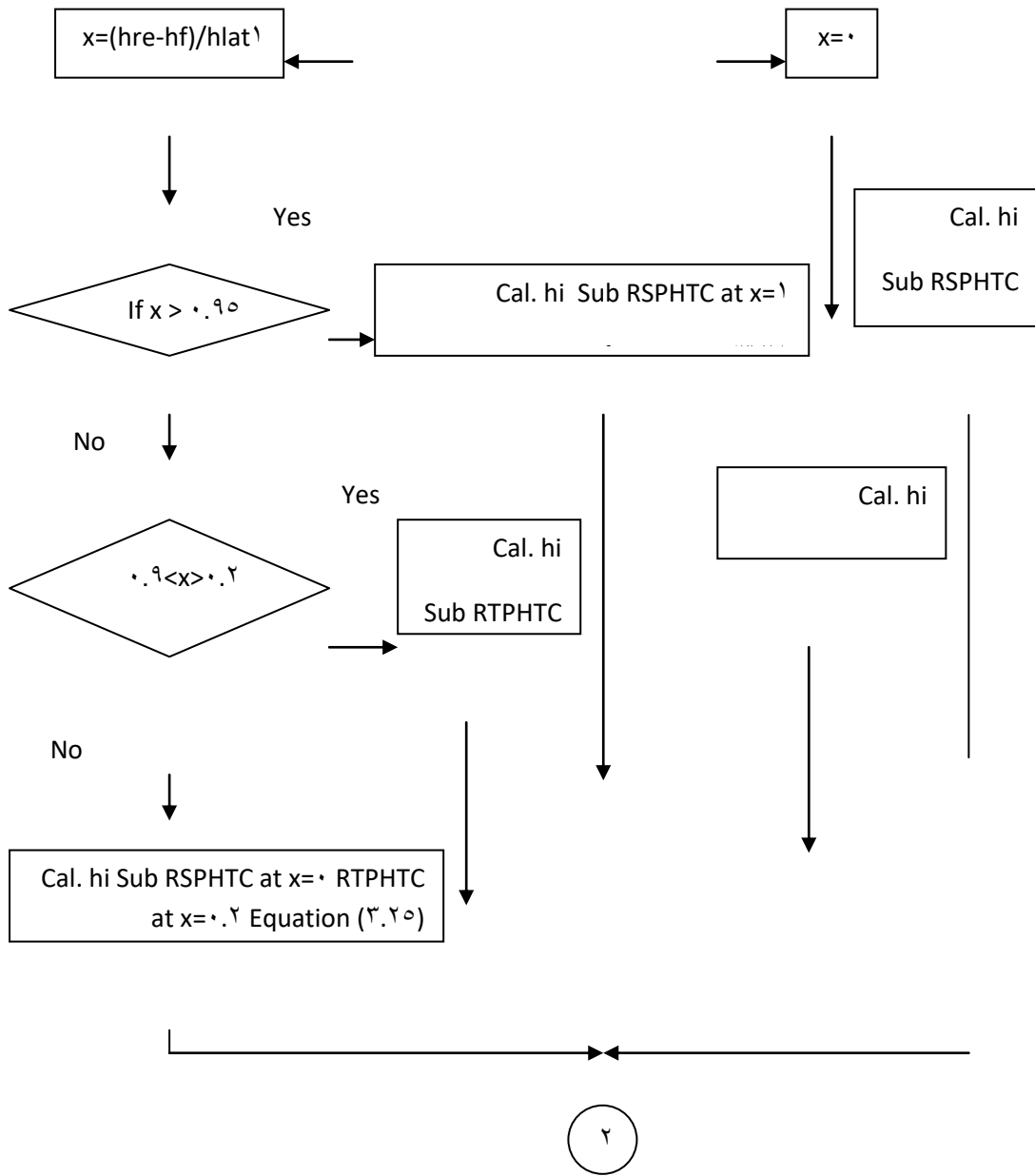
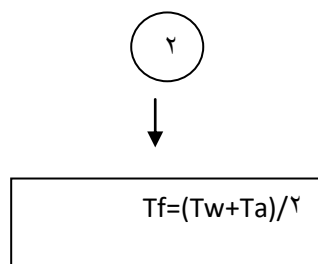
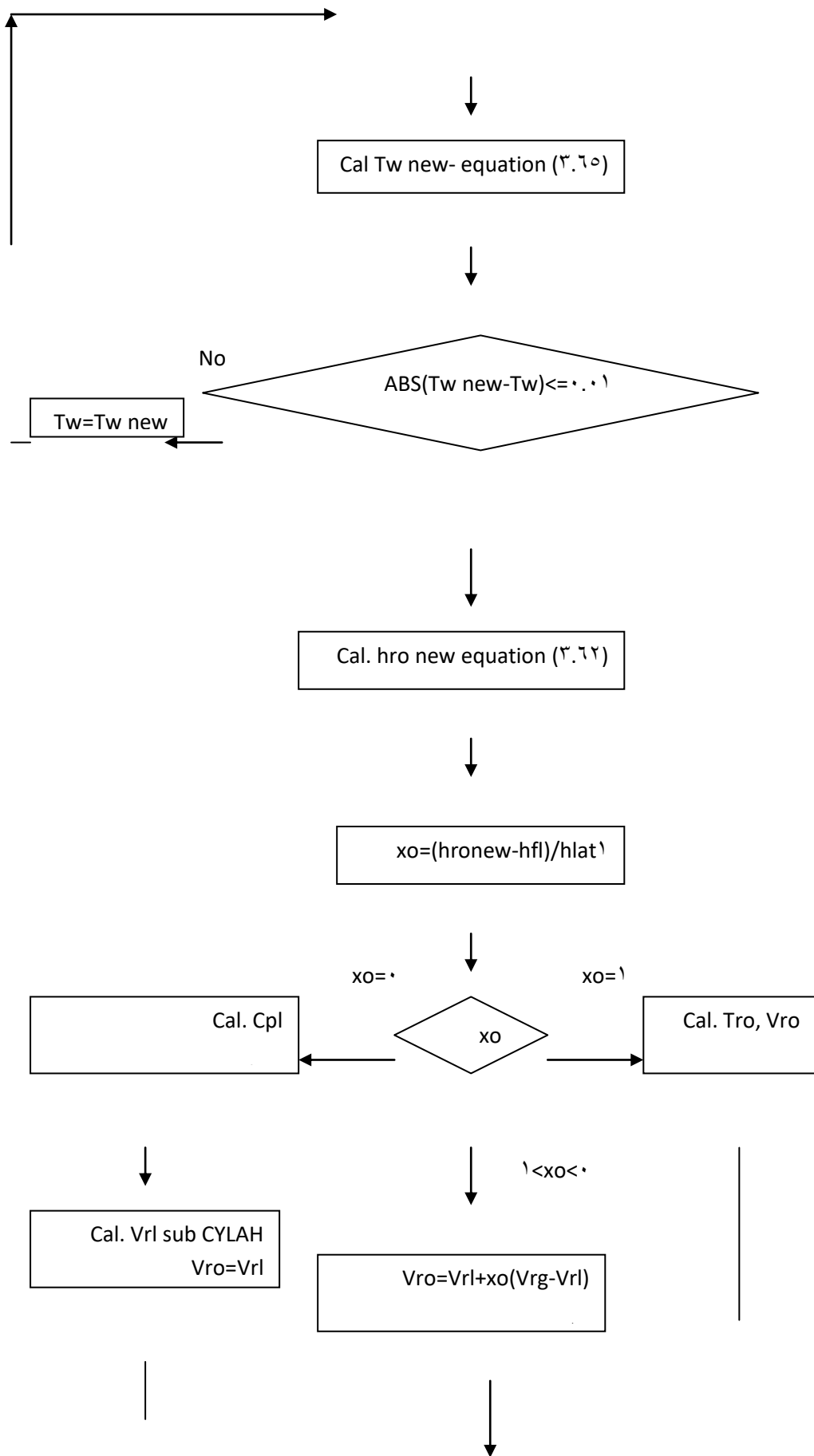


Figure (3-0) continued





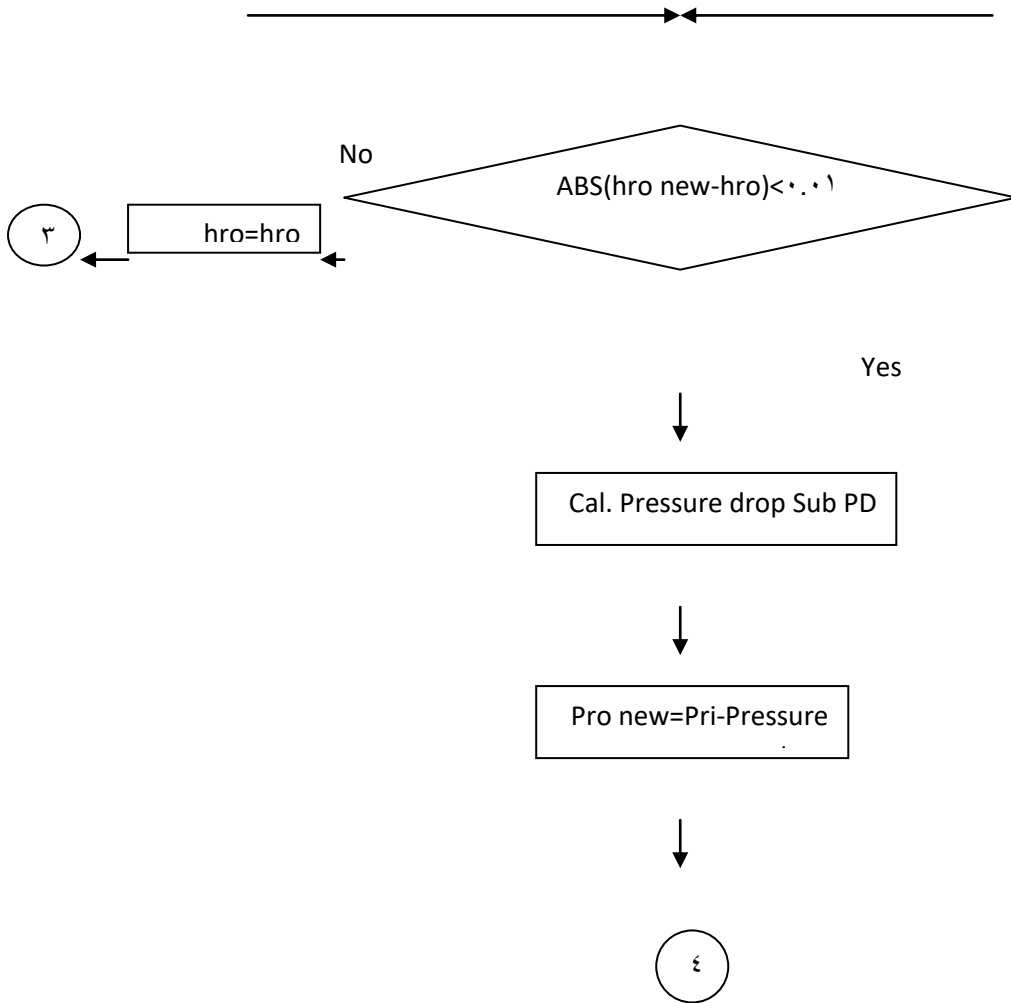


Figure (3-5) continued

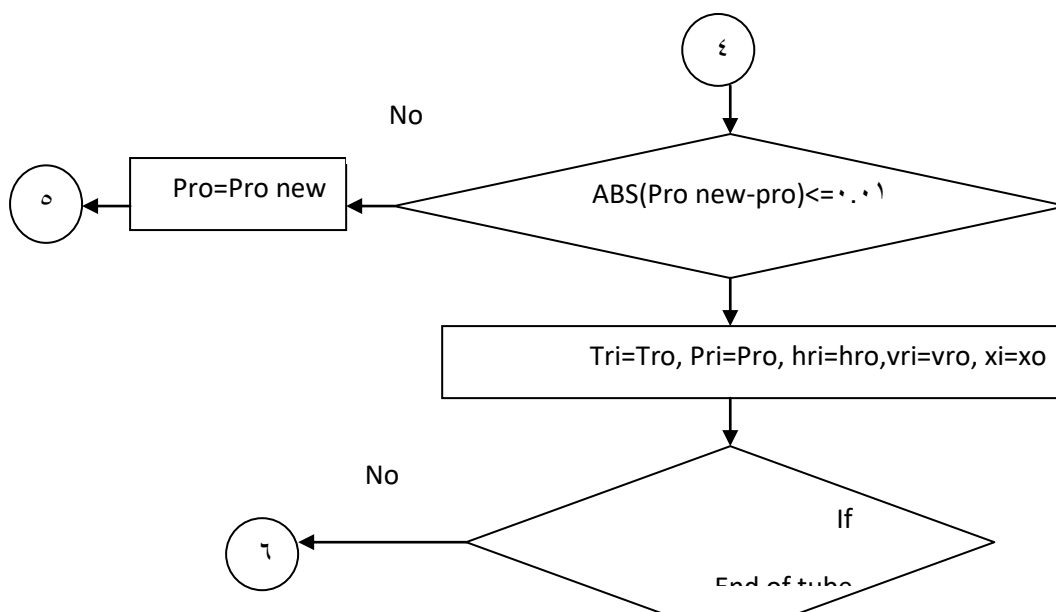


Figure (3-5) continued

EXPEREMENTAL WORK

4.1. Introduction

Theoretical investigations of an actual system have been carried out, from which the relation of: temperature fields in individual components of the refrigerating system, pressure in characteristic places of the system, and active electrical power of the compressor engine as a function of time have been obtained. These results of measurements make it is possible to correlate the model investigations.

The aims of the experimental work are:

1. To test the performance of refrigeration cycle using R134a.
2. To study mainly variables, affect the performance of refrigeration cycle.
3. Experimental results are used to verify the developed model.

4.2. Test Rig Layout

The test rig layout is shown schematically in figure (4-1) and photographically in figure (4-2). It consists of general refrigeration cycle trainer Mod. RCT/EV. The educational panel of this equipment provided with mimic diagram and control board shows an exploded view of all its components allowing an easy study of the thermodynamic cycle of compression refrigeration. This trainer also constitutes the necessary introduction to a complete laboratory for studying and testing refrigeration and air-conditioning

equipment. The phenomena of condensation and evaporation can directly be displayed through some transparent components of the respective exchangers. Direct measurement of temperature and pressure was found in various points of the system it is possible to draw the actual cycle of the refrigerant (HFC R134a) on the pressure-enthalpy diagram and to check its efficiency.

Moreover, it is possible to compare the cycles with expansion through a capillary tube and through a thermostatic valve. The refrigeration cycle equipped with flow meter, sight glass of liquid, humidity indicator and refrigerant driers. Control board is also provided with voltmeter, ammeter and wattmeter, which can constantly check the power consumption of the electrical airtight compressor and of the ancillary equipment.

Then the overall actual efficiency of the system can be found through the measurements of the wattmeter and the use of P-h diagram of the refrigerant.

Therefore the Trainer is particularly suitable for the functional analysis of each component of the refrigeration cycle, for the analysis of their interaction during the operation according to the filling level, for the reconstruction of the actual cycle on the pressure-enthalpy diagram, as well as for the analysis of eventual faults of these components. More details are given by Ref. [19].

4.2.1. Refrigeration Unit.

The refrigeration unit used is essentially a laboratory Elettronica Veneta & INEL SPA refrigeration unit made by an Italy Company, model RCT/EV. It uses a simple vapor compression cycle with R134a as working fluid. The refrigeration unit includes the following parts.

1. Compressor.

The compressor is a closed reciprocating machine, two cylinders within an airtight shell, single stage unit, TR equipment type E11872. Swept volume or piston displacement of 12 cm³ and with a clearance factor of (0.04).

Figure (4-2) shows the cross section of the airtight compressor.

2. Heat Exchanger.

The condenser or evaporator figure (ξ-ξ) is type CA 220/100, model tube of copper 10 mm diameter, pitch of tubes: 20×20 mm, pitch of fins: 20 mm, over length 220 mm, number of tubes ξ. The overall heat exchanger surface is equal to 3.378 m².

The heat-exchange surface of the condenser or evaporator is result of the area of its fins minus the holes for the tubes, plus the surface of the same tubes.

The data of the condenser or evaporator are:

Number of tubes $n = \xi$

Length of tubes $l = 0.22 \text{ m}$

Length of the external elbow $l' = 20 \text{ mm} = 0.02 \text{ m}$

Number of elbows $n' = 2$

Diameter of tubes $\varnothing = 10 \text{ mm} = 0.01 \text{ m}$

Number of fins $N = 66$

Dimensions of fins $D = 0.02 \text{ m} \times 0.02 \text{ m} = 0.0004 \text{ m}^2$

The surface is calculated through the expression::

$$\Delta f_{\text{fins}} = N \times D - [(\varnothing)^2 \times n \cdot n \cdot N] = 3.168 - 0.0004 = 3.168 \text{ m}^2$$

$$\text{Area of tubes } \pi \times \varnothing \times l \times n + \pi \times \varnothing \times l' \times n' = 0.368 + 0.004 = 0.372 \text{ m}^2$$

The overall heat exchanger surface is equal to 3.378 m².

3. Thermostatic Expansion Valve.

The expansion valve is of variable orifice area used before the evaporator as shown in figure (ξ-ϖ).

The adjustment screw to maintain the selected value of the low pressure in the evaporator adjusts the valve manually. The flow coefficient for the orifice, c_{ev} is 0.7 and the valve orifice area is fixed at $0.5E-06 \text{ m}^2$.

ξ. Capillary tubes: The capillary tubes consist of an extremely small-bore tubes of different diameter and length as shown in figure (ξ-ϑ) to study the effects of these parameter on the flow process in the refrigeration cycle.

ξ.ϒ.ϒ. Measuring Instrumentation.

The parameters to be measured during the test are the temperatures, the pressure and the flow rate.

ϑ. Digital thermometers.

Temperature can be monitored at ϑ different locations. The digital thermometers have range of $(-0.0^\circ\text{C}$ to 100.0°C) display 3 digits with sign, accuracy rating $\pm 0.1\text{K}$, as shown in figure (ξ-ϒ).

The digital thermometers used to measure the cold and hot refrigerant at the following location.

- Compressor inlet.
- Condenser inlet
- Five nodes at different location in the condenser.

- Condenser outlet.
- Evaporator inlet.
- Five nodes at different location in the evaporator.

2. Pressure gauges.

Two pointer pressure gauges are used, figure (2-8). One of them is used to measure high pressure which has the range of (0 to 30) bar, and the other to measure low pressure, which has the range of (0 to 10) bar.

3. Flow meter.

The flow meter of variable area type with measuring glass figure (2-9) is used to measure refrigerant volume flow rate. It has range of (0.3-0.3) L/min to measure the circulated refrigerant in the high-pressure line after the condenser.

4.3. Calibration of measuring instrumentation.

The entire measuring devices must be calibrated before the test. In the present work the measuring instrumentations are calibrated by the Electronic Ventura & INEL SPA. More details about function of a calibration of this instrumentation were showed by Elettronicaventa & INEL SPA manual [19]. For more accuracy the calibration processing for digital thermometers to ensure the accuracy of them. The calibration process is satisfied by using three types of experimental materials, these are: die ionized water, Heptan, Acetone and Putanon . The boiling and freezing temperatures for these materials must be known previously. The measured temperature must attain at an instance of absolute or transform conditions from the solid phase (ice) to the liquid phase. After this, the four materials are subjected to heater so that these materials have been found in boiling case. In this instant the temperature must be record again and considered as boiling temperature. These processes are repeated for the four materials so that the results are five points of (three for boiling and other for freezing). Finally, two curves are extracted; one for the experimental measuring and the other for the theoretical values that must be available

previously. These curves are showed in Fig.($\xi-10$) where the x-axis represent the reference value and y-axis represent the measured values and the reading shown in table ($\xi-1$).

Theoretical		Reading
x-axis	y-axis	y-axis
0	0	0.7
06.0	06.0	06.3
79.6	79.6	79.2
100	100	99.81
101.7	101.7	101.08

$\xi.4$. Test Procedure.

Refrigeration cycle Trainer Mod. RCT/EV was used to perform the measurements requirement for individual components of refrigeration system in order to verify the theoretical models of these components.

Initially, the ambient temperature of the laboratory was measured by digital thermometer which was fixed in the system. Also the initial temperatures of all components reading from the screen of these digital thermometers, which were the same in individual position of the test rig. This temperature in all tested conditions, for the condenser and evaporator wall, and refrigerant in the coil is 26°C . At this temperature the condenser and evaporator are both at the saturation pressure and in equilibrium as indicated by the pressure gauge.

The test is standard including measured of, the temperatures at 14 locations mentioned in section ($\xi.2.2.1$), the discharge and section pressures. The volume flow rate of refrigerant was also measured through calibrated flow meter. These

measured values are recorded at τ seconds step time until steady state is achieved.

To simulate the operation with the dynamic refrigerator model, a preliminary run is made from the initial conditions.

In the laboratory, the refrigerator runs to a steady state condition and then shut off with on/off switch and left switch fan on through the condenser and evaporator to reach an equilibrium state. After that the refrigerator is turned on, and data recorded from different measuring devices mentioned in section (4.2.2).

The above tested conditions are repeated many times to obtain a good accuracy of reading recorded.

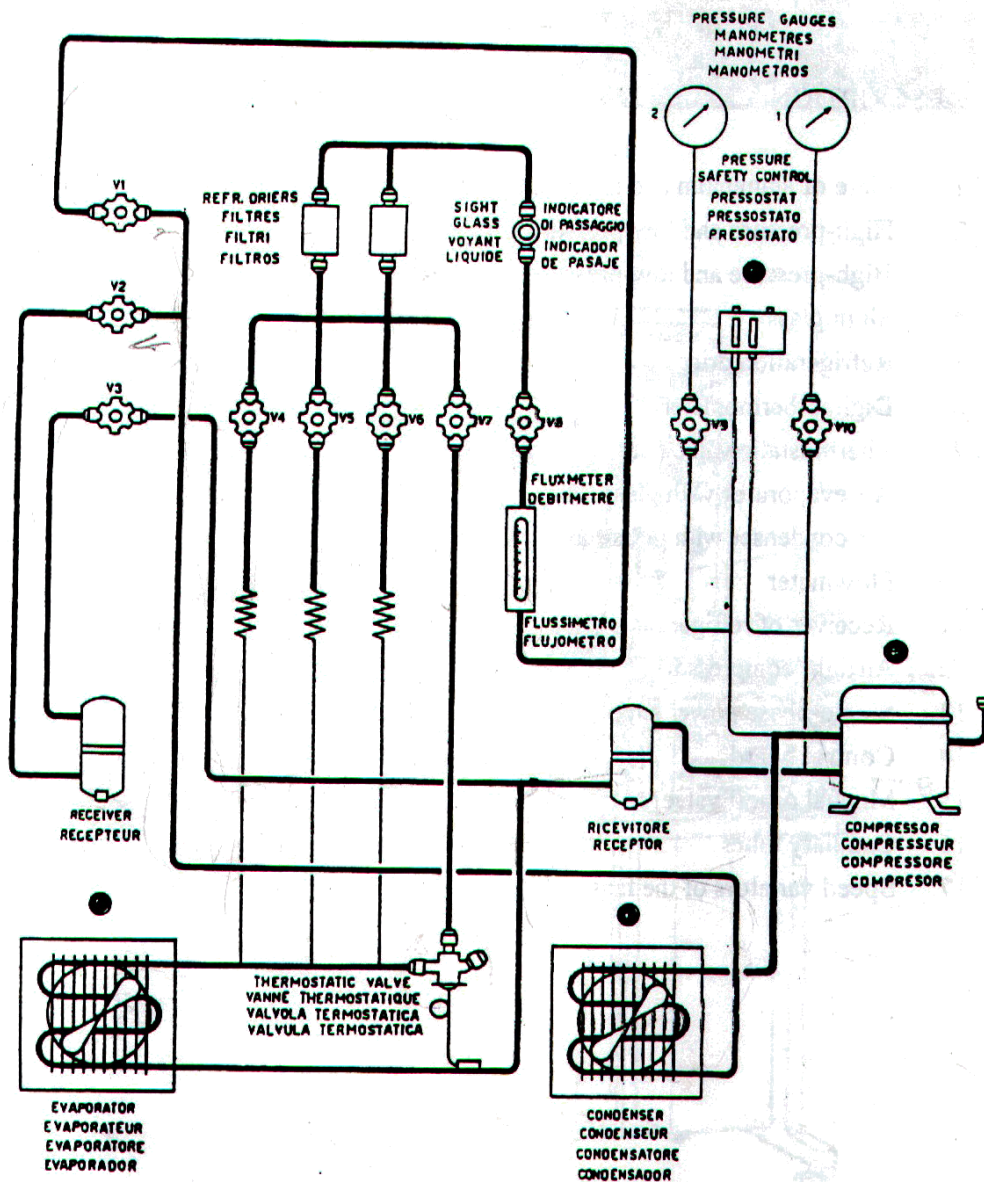


Figure - 4-1

Schematically diagram of the trainer RCT/EV

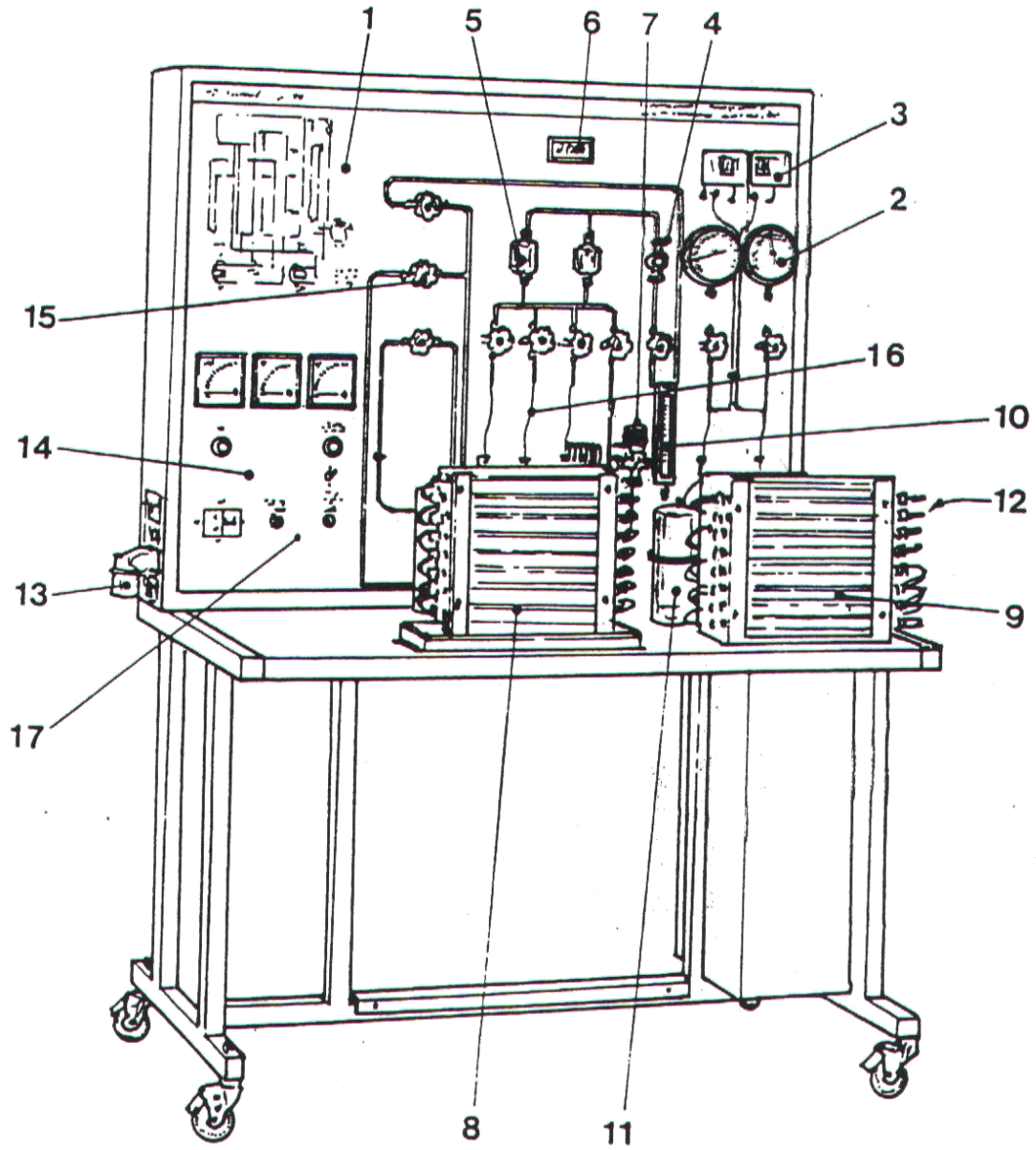


Figure – 4-2

a-Sketch diagram of the trainer RCT/EV

DESCRIPTION

1. Plate of aluminium and mimic diagram
2. High-pressure and low-pressure gauges
3. High-pressure and low-pressure switches
4. Sight glass
5. Refrigeration drier
6. Digital thermometer
7. Thermostatic valve and capillary tubes
8. Air evaporator with glass tubes
9. Air condenser with glass tubes
10. Flowmeter
11. Receiver of refrigerant
12. Airtight compressor
13. Single-phase power supply
14. Control board
15. Manual on-off valve
16. Capillary tubes
17. Speed variators of the fans

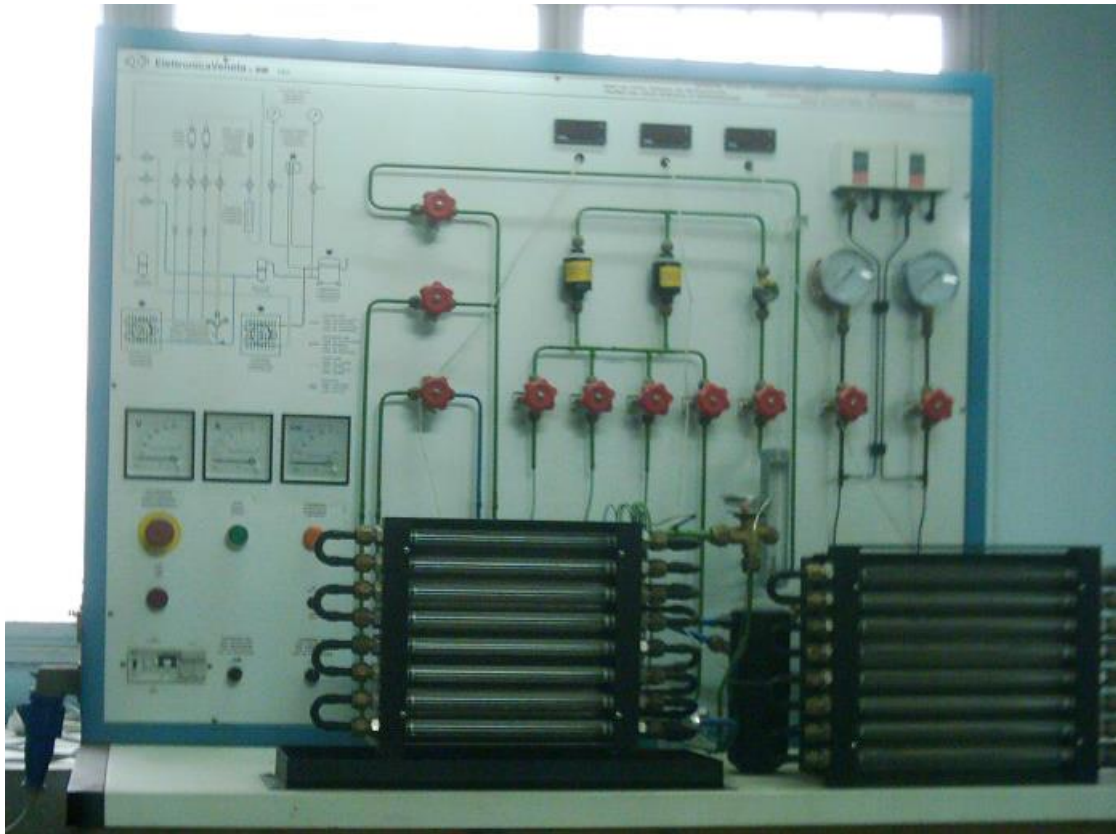


Figure 4-2

b- Photographically diagram of the trainer RCT/EV

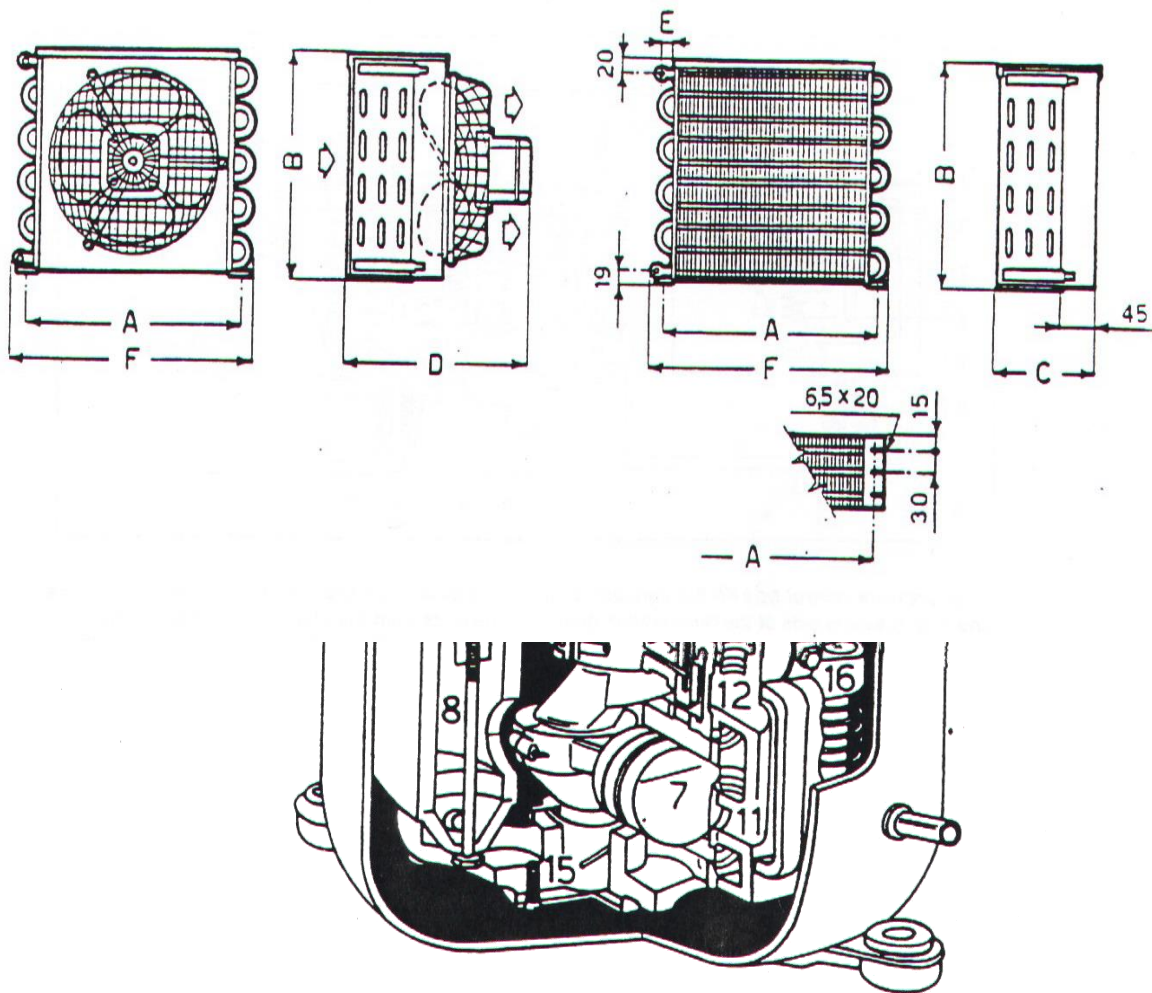
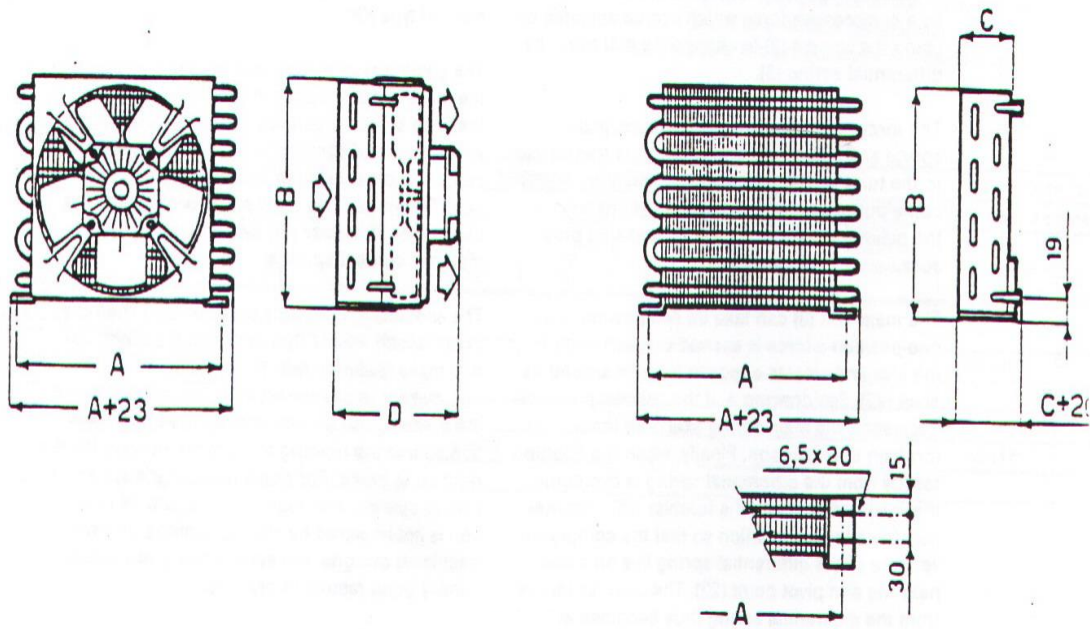


Figure 4-3

Cross section of an airtight compressor

- | | |
|------------------------------------|---|
| 1. Stator of the electric motor | 11. Suction manifold |
| 2. Rotor of the electric motor | 12. Suction and exhaust valves
(superimposed and coaxial) |
| 3. Winding | 13. Exhaust silencer |
| 4. Sensor of the thermal protector | 14. Exhaust pipe |
| 5. Drive shaft | 15. Lubricant suction |
| 6. Main bushing | 16. Elastic suspension of the
machine within the airtight shell. |
| 7. Piston | |
| 8. Suction chamber | |
| 9. Suction silencer | |
| 10. Suction pipe | |

a – Evaporator



b – Condenser

Figure 4-4

Heat exchanger (Condenser and Evaporator)

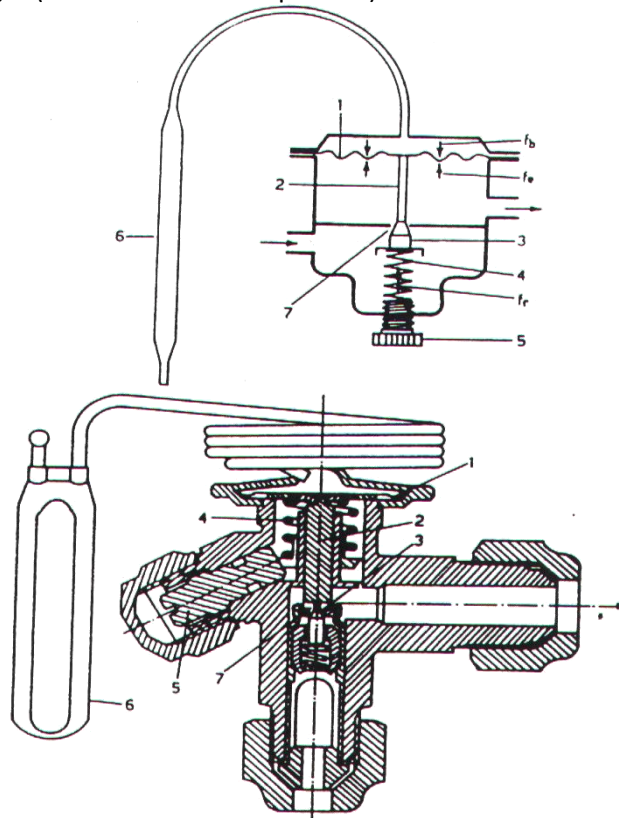


Figure 4-5

Thermostatic expansion valve

- 1. Orifice meter
- 2. Control tappet
- 3. Shutter
- 4. Adjustment spring
- 5. Adjustment screw
- 6. Bulb
- 7. Orifice

f_b Force exerted by the fluid of the bulb

f_e Force of the gas pressure at the evaporator inlet

f_r Force of the adjustment spring

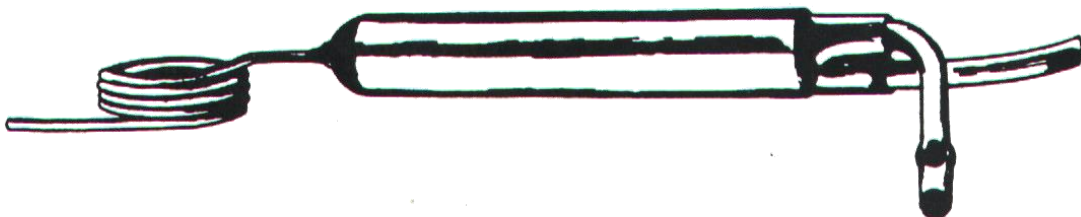
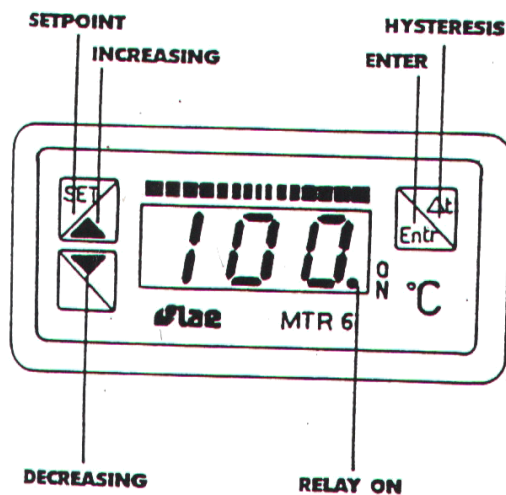
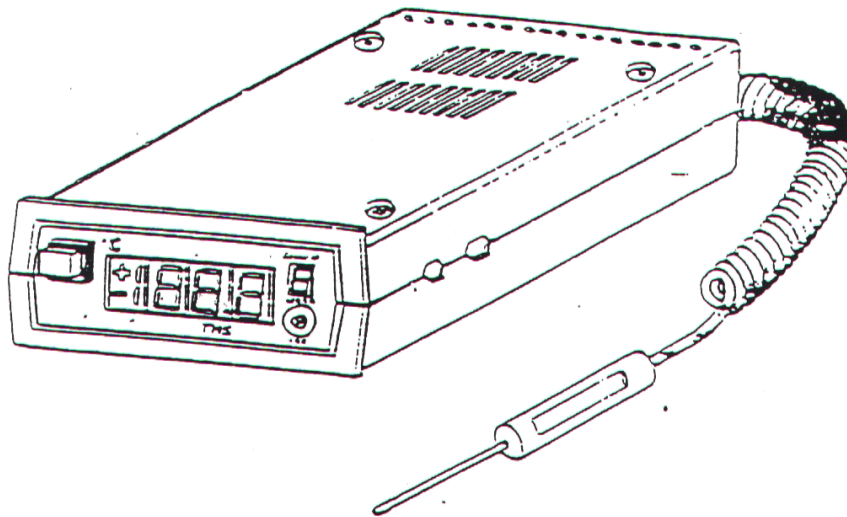


Figure 4-6

Capillary tube



**TECHNICAL DATA Mod. MTR6 T1 RD
MTR6 T1 RD**

Dimensions	64x32 mm.
Measuring range	-50 °C to 150 °C
Display	3 digits with sign
Accuracy rating	±1 °K
Resolution	1 °C
Type of sensor	PTC 1000 Ω - 25 °C
Probe connection	with 3 wires
Operating temperature	-10 °C to 60 °C
Storing temperature	-30 °C to 80 °C
Interference susceptibility:	standard IEC 801
Type of relay	SPDT; 300 Va.c. Max
*Defrosting relay	SPST; 300 Va.c. Max
Switchable power	1800 VA; 170 W
Connections:	terminal board max. Ø 4 mm ²
Power supply	12 Va.c./d.c. ± 10%
Consumption	2 VA max

Figure 4-Y

Digital thermometer

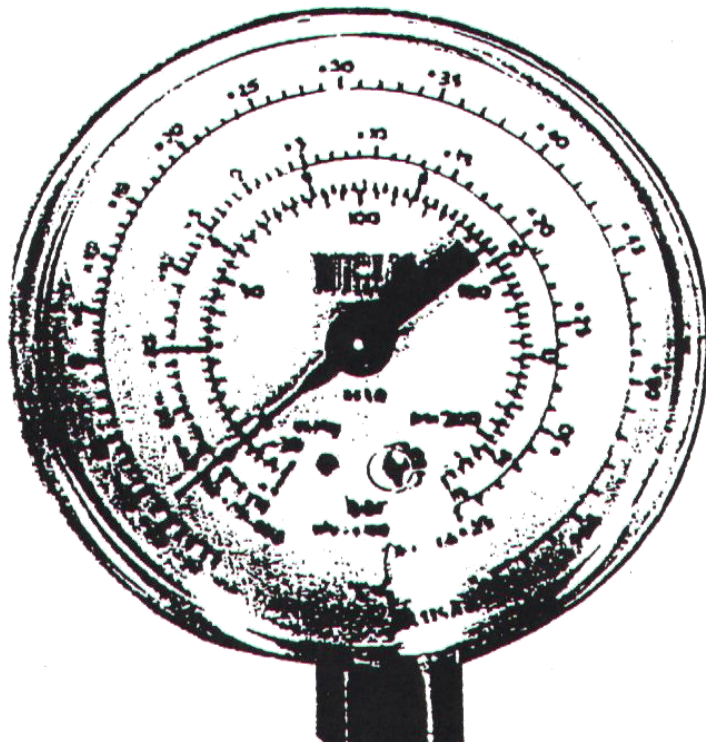
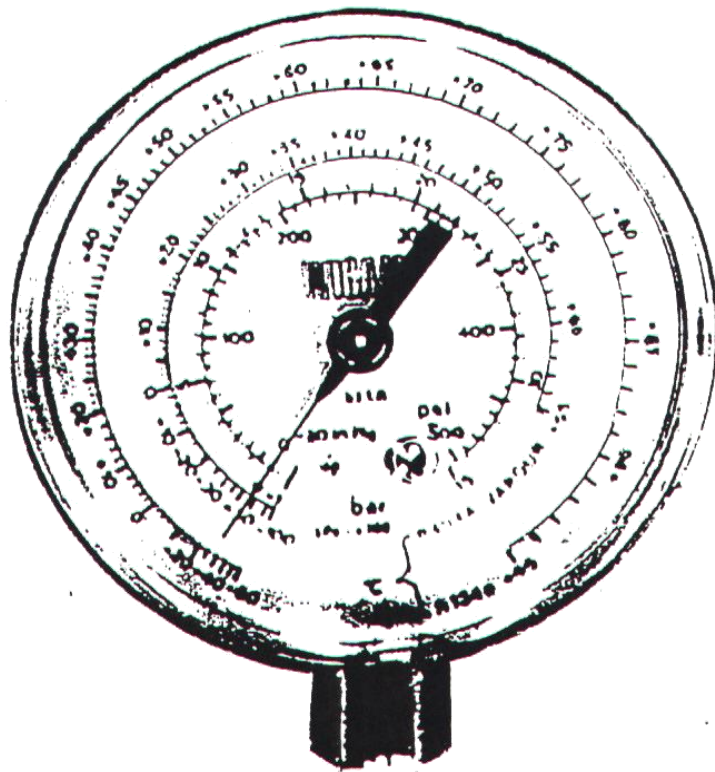


Figure 4-8

High - Pressure and low - Pressure gages

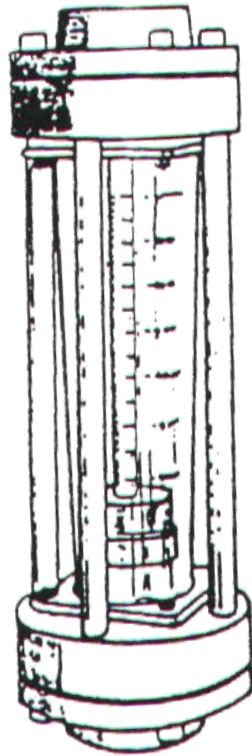


Figure 4-9

Flow meter

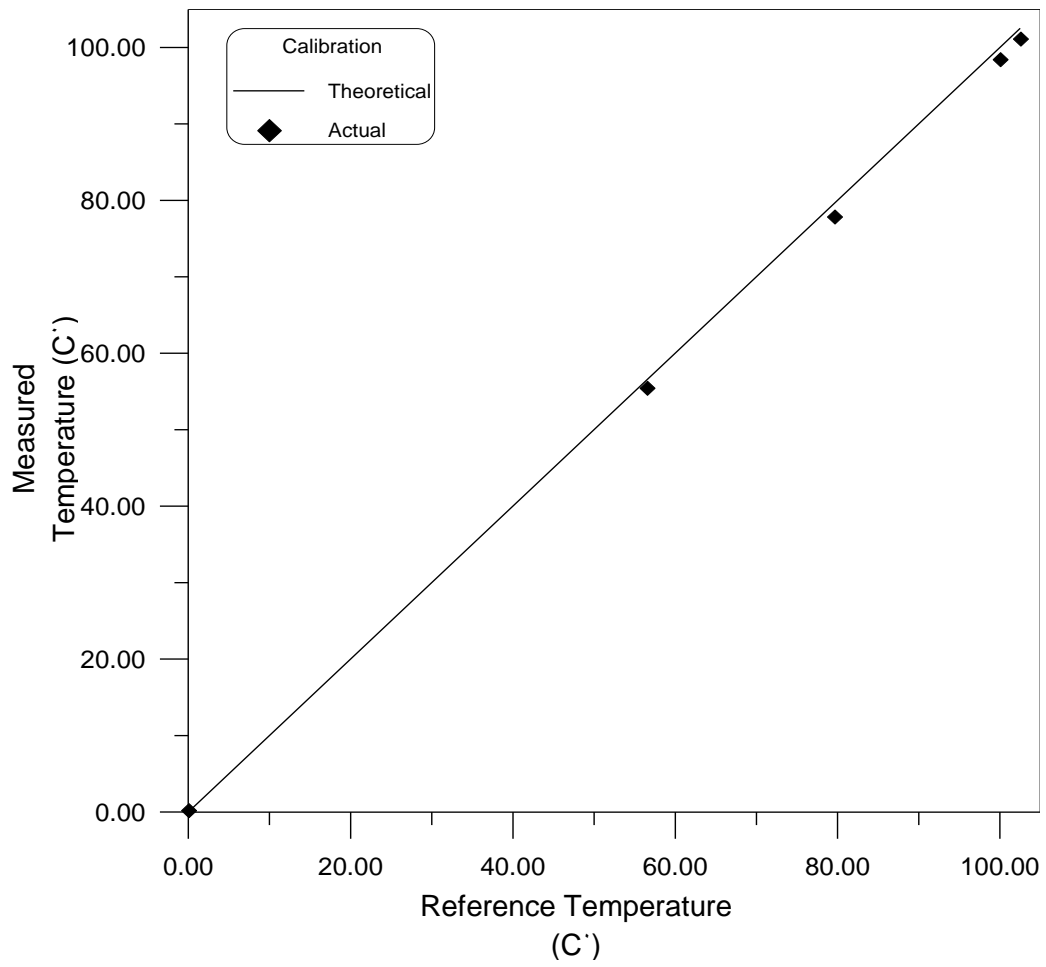


Figure 4-10 : Calibration of digital thermometers